# Is spectral pixel-to-pixel variation a reliable indicator of grassland biodiversity? A systematic assessment of the spectral variation hypothesis using spatial simulation experiments

Antonia Ludwig[1,2,3,*], Daniel Doktor[1,2,4], and Hannes Feilhauer[1,2,3,4]

[1]Helmholtz Centre for Environmental Research - UFZ Leipzig, Permoserstraße 15, 04318 Leipzig

[2]Remote Sensing Centre for Earth System Research - RSC4Earth

[3]Leipzig University, Institute for Earth System Science and Remote Sensing, Talstraße 35, 04103 Leipzig

[4]German Centre for Integrative Biodiversity Research - iDiv Halle-Jena-Leipzig, Puschstraße 4, 04103 Leipzig

[*]Corresponding author: antonia.ludwig@ufz.de

## Abstract

Covering 30 - 40% of the terrestrial surface, grasslands are important hosts of biodiversity, crucial for nutrient cycles and carbon sequestration. However, these ecosystems face a pressing threat in the form of biodiversity loss, which can disrupt their functioning and resilience. Addressing this challenge requires effective monitoring of biodiversity changes on large scales. Remote sensing emerges as a valuable tool in this endeavour, enabling the assessment of grassland biodiversity through the analysis of vegetation patterns, species composition, and ecosystem health over extensive areas.

According to the spectral variation hypothesis (SVH), the link between pixel-to-pixel spectral variation and species diversity in remote sensing images can be used to retrieve plant diversity based on spectral data. Nevertheless, the transferability of the proposed relation across ecosystem types, seasons and spatial resolutions remains unclear. The absence of comprehensive data has hindered systematic assessments of the SVH so far, which would ideally incorporate coherent sets of diversity estimates from remote sensing data and in-situ plant diversity measurements.

With this study, we present a combined approach that brings together trait data from field measurements, simulations of spatial species distributions and radiative transfer models for a systematic and

in-depth analysis of the SVH in temperate grasslands. Based on simulated grassland communities with different diversity levels, we assessed the spectral-to-species diversity relationship across (1) three temperate grassland types, (2) three seasons and, (3) five spatial resolutions (from 10 m to 0.2 m pixel size). We used the mean Euclidean distance (mED) and Rao's Q as measures for spectral diversity and different indices to describe the species and trait diversity of the simulated grassland communities.

Based on 45000 simulated grassland communities in five different spatial resolutions, we found that the spectral-to-species diversity relationship is not stable across grassland types and seasons, despite the used spectral diversity metric. Correlations with spectral diversity were inconsistent for the different applied diversity indices and no single index outperformed the others. Spectral diversity was mainly driven by the spatial resolution (i.e. pixel size) of the image and not by species richness (SR) or functional trait diversity (FD) per se. Our results further underline that the link between SR and FD is not always prominent in plant communities and the basic assumption of the SVH is fulfilled only under certain conditions. Consequently, we argue that FD, which is an important driver of the spectral signature of a plant community, is not inevitably linked to the number of present species in an image. We conclude that the interplay of SR and FD is crucial for the expression of the spectral-to-species diversity relationship. This study clearly underlines the context-dependency of the SVH and we point out that, although of promising value for distinct ecosystems, it is not universally applicable.

***Keywords***— spectral heterogeneity, vegetation remote sensing, species richness, functional diversity, radiative transfer models, spatial resolution

# 1 Introduction

Biodiversity is declining globally at incomparable rates and across all types of ecosystems (Díaz et al. 2019). This loss is associated with dramatic effects on ecosystem functions and services that provide the basis for global cycles and human well-being (Cardinale et al. 2012). Plant diversity plays a crucial role in the maintenance of ecosystem stability, productivity and health and is therefore of special interest for the monitoring of ecosystems under climate change (de Bello et al. 2021; Hautier et al. 2015). Covering around 30 - 40% of the terrestrial surface, grasslands are the most intensively used land-cover type (Gibson 2009). By hosting a large variety of plant species and providing habitats to other organisms, they are of utmost importance for the maintenance of global biodiversity. Further, they provide essential carbon sinks and therefore contribute substantially to mitigating global warming caused by carbon emissions (Petermann et al. 2021).

Earth observation data play an important role in the development of tools to quantify plant diversity continuously across large spatial scales. In-situ measurements of plant diversity are time and labour intensive, restricted to a limited spatial extent and the trade-off between time and observation area

needs to be considered carefully. They are further biased by the seasonal occurrence of the plants, the accessibility of the field site and the experience of the observer (Burg et al. 2015). Considering the limitations of traditional vegetation surveys, the additional application of remote sensing (RS) techniques can provide a helpful expansion. According to a review of Wang et al. (2019), the assessment of plant diversity from RS data can be differentiated into four groups: (1) indirectly through habitat mapping, (2) directly through the mapping of individual plant distributions, (3) the mapping of functional diversity (based on plant traits, which are more closely related to ecosystem functioning than the species per se), and, (4) based on spectral variability. Recognising the value of all mentioned methods, we focus on the retrieval of grassland diversity based on spectral variability in this study.

Introduced by Palmer et al. (2000), the Spectral Variability Hypothesis (SVH) in its original version states that the spectral variability of an RS image is linked to the species richness (SR) of the captured area. Spectral variability (or spectral diversity) describes the quantitative differences in the reflectance spectra between the spatial units (pixels) in a RS image. The basic SVH assumption is that increased spectral variability reflects an increased variety of habitats in the surveyed area and a higher number of habitats can harbour more species. Accordingly, spectral variability, which indirectly reflects the diversity of habitats, can be used as an indicator for SR (ibid.). Over the years, the SVH passed through a scientific development in which both its name (towards Spectral Variation Hypothesis) and both the response and explanatory variables evolved continuously. The assumed spectral-to-species diversity relationship has been applied to RS data in order to assess not only SR (Hall et al. 2012; John et al. 2008; Lucas et al. 2010; Rocchini, Duccio 2007) but also other related diversity measures, such as species diversity (SD, Hauser et al. 2021; Heumann et al. 2015; Oldeland et al. 2010; Wang et al. 2018b) or functional diversity (FD, Pacheco-Labrador et al. 2022; Schneider et al. 2017; Schweiger et al. 2018). These are three among an ample variety of measures that provide different perspectives on biodiversity. The metrics are often used jointly to gain a comprehensive understanding of ecosystem health and stability. In summary, SR quantifies the total number of species, SD considers both species richness and their relative abundance, and FD evaluates the variety and variability of functional traits and roles exhibited by species. Recent studies have shown that the use of different biodiversity measures can lead to different outcomes regarding the strength of the spectral-to-species diversity relationship (Hauser et al. 2021; Pacheco-Labrador et al. 2022). The choice of the most appropriate measure of spectral diversity is an object of ongoing discussion. Among the most commonly applied indices are the mean Euclidean distance (mED), Rao's quadratic entropy (Rao's Q, Rocchini, Duccio and Marcantonio, Matteo and Ricotta, Carlo 2017), the coefficient of variation (CoV), and the standard deviation. All four indices are quantitative measures that provide insights into the distribution of spectral data. Higher values of each index generally indicate greater spectral diversity, while lower values suggest lower diversity. Rao's Q considers both richness and evenness, while the other indices focus primarily on dissimilarity or variation. mED calculates pairwise dissimilarities, while standard deviation measures absolute variability and CoV assesses relative variability by normalising it with respect to the mean. mED and Rao's Q are multivariate metrics that

are more suitable for hyperspectral data, whereas CoV and standard deviation are univariate metrics that account for single bands only. Consequently, they require substantial dimensionality reduction and are not suitable to reflect the variability of hyperspectral data in the mulitdimensional space.

### Drivers of spectral variation

The reflectance patterns of plant communities are governed by a combination of physiological, anatomical, and biochemical characteristics of the plants. These factors interact with incident light across different wavelengths of the electromagnetic spectrum, leading to distinctive reflectance patterns that can be captured by remote sensing technologies. Plant canopy reflectance is driven by the set of plant traits that cover the above-ground parts of plants which can be referred to as *optical plant traits* (G. P. Asner 1998; Cavender-Bares et al. 2017). Depending on the spatial resolution of the sensor, the received signal is composed by more or less mixed reflectances of several plant individuals and the background reflectance. We can assume that this signal is mainly determined by the dominant species in the plant community. According to the SVH, we expect a higher spectral variability for areas with higher SR and consequently a more diverse set of optical traits. Recent studies pointed out that species and their optical traits are not the only important drivers for spectral variation in RS images. Other important factors are (1) vegetation cover (Hauser et al. 2021), (2) habitat type (Perrone et al. 2023; Rossi et al. 2022), (3) the spatial distribution patterns and abundances of the species (Fassnacht et al. 2022; Wang et al. 2018a), (4) the seasonal development of the vegetation (Thornley et al. 2022; Wang et al. 2016), (5) and the spatial resolution of the RS data (Rocchini, Duccio 2007; Wang et al. 2018b). Of particular importance is the vegetation cover, since background soil reflectance can have major effects on the optical signal and can lead to an increase of spectral diversity which might cause an overestimation of SR (Gholizadeh et al. 2018; Hauser et al. 2021; Wang et al. 2019). Further, the spatial distribution patterns of different species in the prevailing plant community influence the spectral variation in remote sensing images. Some species, such as *Tanacetum vulgare*, grow in patches while others, such as *Lolium perenne*, are distributed homogeneously. This causes local variations in the vegetation composition across an area, with 'hotspots' of species and trait density in some patches. Spatially heterogeneous trait distribution patterns are locally expressed in the reflectance patterns and increase the spectral variability. These patterns are enhanced by the variety of life forms in grassland ecosystems. Different species of a grassland community can exhibit a large variation in size and growth types (such as grasses, herbaceous species, small shrubs, Petermann et al. 2021). Woody species, such as *Calluna vulgaris*, introduce an additional effect of bark (non-greenish plant material that is not part of dead vegetation) to the spectral reflectance pattern and thereby increase spectral diversity.

Beyond different spatial distribution patterns, the species of a plant community occur in different proportions (i.e. 'species abundances'). Recent studies have shown that spectral diversity is influenced not only by species SR but rather by the interplay of SR and the single species abundances (i.e. 'evenness' of a community) (Rocchini et al. 2014; Wang et al. 2018b). Abundance-weighted diversity indices,

such as Simpson's (Simpson 1949) or Shannon's index (Magurran et al. 2010), express stronger links to spectral diversity than SR (Wang et al. 2018a). This can be explained by the fact that the sensor receives a mixed spectral signal that contains the spectral signatures of all plant species in a pixel. This mixed signal is mainly driven by the most dominant plant species, which is more appropriately reflected using abundance-weighted diversity indices. Additionally, seasonal effects influence the spectral-to-species diversity relationship. Throughout the seasons, temperate grassland communities exhibit changes in their species composition, vegetation structure and trait phenological conditions. Recent studies have reported that the timing of sampling has a strong effect on the spectral-to-species diversity relationship (Thornley et al. 2022) and should therefore be considered in diversity assessments based on RS data. Further, different management practices must be considered when assessing grassland diversity from RS data as these change the phenological condition and structure of an area independently from the seasonal cycle (Rossi et al. 2022). Finally, the spatial resolution of the RS image (i.e. pixel size) plays a major role in the spectral-to-species diversity relationship (e.g. Rocchini, Duccio 2007; Rossi et al. 2022; Wang et al. 2018b). The ratio between the size of a pixel and the observed objects determines the degree to which the received spectral signal is a mixture of different reflectance spectra (Cavender-Bares et al. 2017). This is especially apparent in grasslands where the pixel size and the individual plant size can differ considerably (Rocchini et al. 2022). Depending on the applied sensor and observed life form, small pixels can already contain a mixture of several plant individuals. Wang et al. (2018b) therefore recommend a spatial resolution from 1 mm to 10 cm for the assessment of herbaceous plant diversity. However, such fine resolutions are only achieved by drones, which do not meet the requirements for large-scale coverage for diversity monitoring. All these parameters are fundamental drivers of spectral variation in RS images. Unfortunately, they rarely occur exclusively and their single effects on spectral variability are hard to disentangle. Although presenting a promising and straightforward approach in times of urgently needed grassland diversity monitoring, we should acknowledge that the SVH exhibits various weaknesses (see also Fassnacht et al. 2022; Schmidtlein et al. 2017). A detailed analysis of the effects of different drivers on the spectral-to-species diversity relationship in grasslands on large scales is a challenging venture. This is mainly caused by strong practical limitations in the experimental design. On the one hand, exhaustive datasets to test the coherence of diversity estimates from remote sensing signals with in-situ measurements of plant diversity are scarce. On the other hand, to analyse the influence of sensor-induced scaling effects, tremendous data processing efforts are required. These are usually avoided due to limitations in human and financial resources.

### Simulation studies to bridge the data gap

A promising approach to fill this gap is the targeted design of simulation experiments that allow to produce a large number of artificial plant communities. Coupled with spectral data or radiative transfer models (RTMs) to generate the spectral data, plant community simulations are a powerful tool to increase the size of the test data and bridge the gap between field observations and RS data. However, recent

studies have shown that the use of pure spectra from leaf measurements (i.e. via leaf clip, Zhao et al. 2021) does not lead to reliable results as the soil reflectance and effects of volumetric scattering cannot be taken into account, although background soil reflectance has been shown to have a strong impact on the spectral variability (Gholizadeh et al. 2018). Additionally, the precise combinations of traits, species diversity, and vegetation cover responsible for the observed spectral variations from air- or space-borne measurements remain unclear, unless these data can be aligned with in-situ measurements (Badourdine et al. 2022). Due to restrictions in the experimental design, none of the studies considered the effects of spatial species distributions in combination with in-situ measurements of plant traits. The spatial plant species distribution across a habitat can lead to different spectral reflectance patterns. Let us compare a uniform plant distribution with stable cover percentages with an area where species are clustered and occur in varying proportions. Depending on the spatial resolution we consider, the first area will exhibit a uniform spectral signal, while the latter will inherently display greater spectral diversity. Consequently, including the spatial plant distribution and corresponding traits in the study design might improve the SVH assessment.

In this study, we present a combined approach that brings together trait data from field measurements, simulations of spatial species distributions and RTMs for a systematic and in-depth analysis of the SVH in temperate grasslands. For this purpose, we collected species data and performed in-situ trait measurements of biophysical properties from three different grassland types in Germany: a nutrient-poor, a nutrient-rich and a dry grassland area. The biophysical properties of these grasslands were measured in spring, summer and autumn 2021 to capture the site- and season-specific aspects of the prevailing plant community in the respective areas. Based on the species data (full vegetation survey including species abundances), we simulated two-dimensional spatial plant distribution patterns that represent artificial grassland communities on a fixed area of 30 m $x$ 30 m. In combination with our trait database, we parameterised a leaf- and canopy-RTM (PROSAIL, Feret et al. 2023; Jacquemoud, Stéphane and Verhoef, Wout and Baret, Frédéric and Bacour, Cédric and Zarco-Tejada, Pablo J and Asner, Gregory P and François, Christophe and Ustin, Susan L 2009) to generate season- and site-specific canopy reflectances according to the grassland simulations. Using this large set of simulations as model landscape patches, we systematically assessed the spectral-to-species diversity relationship across (1) three different temperate grassland types, (2) three seasons and, (3) five different spatial resolutions (from 10 m to 0.2 m pixel size, in line with real-world space- and airborne sensors). We used the mean Euclidean distance (mED) and Rao's Q as measure for spectral diversity and different indices to describe species and trait diversity of the simulated grassland communities.

## 2 Materials and Methods

We used simulated spatial distributions of plant communities based on field observations to test the spectral-to-species diversity relationship in temperate grasslands for different spatial resolutions. Traits

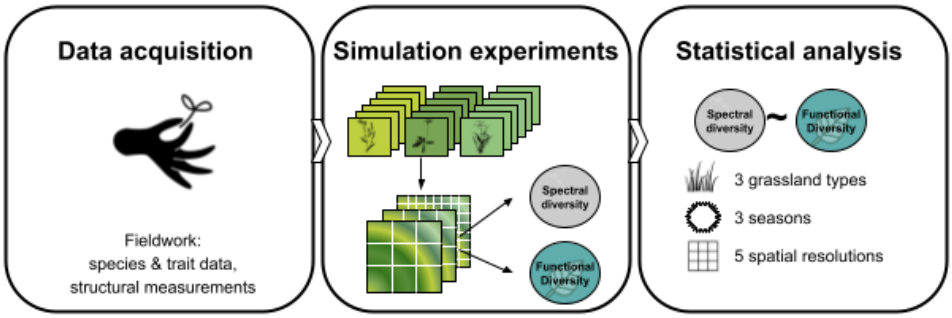


Figure 1: General workflow from species and trait sampling, over grassland simulations and spectra generation to statistical analysis. Species and trait data were collected for three sites and in three seasons, respectively. The simulations were performed for five different diversity levels (5 to 25 species) and with 1000 different species composition variations per diversity level. Spectra were generated by passing the pixel-wise mean trait values to PROSAIL, for the same grassland simulation represented in five spatial resolutions (10 m to 0.2 m pixel size). Based on the pixel-wise reflectance values, spectral diversity was calculated (mean Euclidean distance and spectral Rao's Q). Measures for taxonomic and functional diversity were calculated for every single grassland simulation based on the incorporated species information and trait values. Finally, we calculated the correlation coefficients between the different spectral diversity metrics for Species Richness (SR), Shannon-Index, Simpson-Index and Rao's Q to test the bivariate relationships between multiple variables at different pixel sizes.

from in-situ measurements were used to parameterise radiative transfer models (RTMs) with coherent site- and season-specific trait data. Using pixel-wise optical trait means, we applied PROSAIL to simulate the spectral reflectance of the simulated grasslands (Fig. 1). The species and trait information together with the spectral reflectance patterns were finally used to test the spectral-to-species diversity relationship. All simulations, further calculations and statistical analyses were performed in R version 4.1 (R Core Team 2020).

# Field Work

## Field sites

Samples were collected in three structurally different grassland sites in the surroundings of the cities of Leipzig (Saxony, Germany) and Halle (Saxony-Anhalt, Germany): (1) The Luppeaue (LA, 51°31'7.8"N, 11°53'19.9"E, nutrient-poor grassland), (2) Bad Lauchstädt (BL, 51°23'26.4"N, 11°52'35.9"E, nutrient-rich), and (3) the Lunzberge site (LU, 51°31'45.2"N, 11°53'25.9"E, dry grassland). A more detailed description of the sites can be found in Ludwig et al. (2022).

## Soil reflectance, vegetation surveys & trait sampling

Measurements on each field site were carried out at the end of April, July and September 2021. To minimise the observer bias, the surveys were always performed by the first author. In order to represent the site-specific soil reflectance differences in our simulation experiments, soil samples were collected from all field sites and respective reflectance spectra measured using the contact probe of a field spectrometer (ASD FieldSpec 4®, Malvern Panalytical, UK) in the lab (Fig. A.10). To maximise the effect of background soil reflectance, we included dry soil spectra in the RTMs.

Further, species and trait data were collected from the three field sites to create a database for the grassland simulation experiments. The vegetation surveys and trait sampling were designed in order to assess the typical dominance aspects of the prevailing vegetation of each site. Plant traits were chosen in accordance with the PROSAIL input parameters that was later used to simulate community-specific canopy-level reflectances (Fig. 1). To conduct the vegetation surveys, we recorded all species present within a 2 m $x$ 2 m survey frame. This frame was placed randomly 20 times across the study sites. Plots were at least 5 m apart from each other. Edge zones of the sites were avoided to allow for a continuous species composition and to exclude new species from neighbouring habitats. In each plot, we recorded the cover fraction of all species present within the frame and the overall cover fractions of green vegetation, and bare soil. Coverage was estimated as total cover fraction on a scale from 0 – 100 %. For each species in a plot, the vegetative status was recorded (brown or photosynthetic active) as well as their affiliation to mono- or dicotyledons.

**Leaf- and plant-based measurements**

We collected ten plants per species at each field site and during three seasons. To account for intra-specific trait variability (ITV), we processed each plant sample individually. We measured the Equivalent Water Thickness (EWT, in cm) and Leaf Mass per Area (LMA, in g/cm$^2$) for each plant following Perez-Harguindeguy et al. 2016, excluding petioles and thick nerves. The trait values were later transformed to fit the unit-specific requirements of PROSAIL (Tab. 1).

We determined leaf pigments using two sample sets in order to enhance the accuracy. First, we collected a calibration set of ± 160 leaf samples. For each sample, we used a handheld SPAD-Chlorophyll meter (SPAD-502, KONICA Minolta) to measure SPAD-values as proxy of leaf greenness. The same leaf sample was instantly stored at - 74 °C in the field and later chemically analysed to determine chlorophyll a, b (Cab) and carotenoid contents (Car) through photospectrometry in the lab. This calibration set was necessary, because the precise chemical determination of pigments requires different processing compared to the measurements of leaf traits using fresh leaf material. Additionally, we measured the leaf SPAD-value of each species in the plot. Leaf nerves, senescent or necrotic parts were carefully avoided. We used the average of five measurements per leaf while still being attached to the plant as a species-specific SPAD-value and did this for three leaves per plant. We transformed SPAD-values into total leaf chlorophyll content using typical calibration equations that are based on chemical determination (Markwell et al. 1995). Further, we assessed the deviation of the SPAD-values to the chemically determined Cab based on the calibration sample set and included this deviation in our SPAD-value transformation in order to enhance the accuracy of the SPAD transformation (for more details see Ludwig et al. 2022). Car contents cannot be directly derived from SPAD-values. Instead, we used the calibration set to calculate the Cab:Car ratio and then derived Car contents from the SPAD-based Cab values.

### Canopy-based measurements

In order to obtain structural parameters for the RTM, we measured the Leaf Area Index (LAI) and the Mean Tilt Angle (MTA) using an LAI-2200C (Plant Canopy Analyzer®, LiCor® Biosciences Inc., USA) in each plot. The LAI is a unitless index that corresponds to the accumulated one-sided leaf area per area on the ground and can be treated as indicator of vegetation density. The denser the vegetation cover, the higher the LAI. The MTA is the mean leaf angle distribution of the vegetation within a plot. Both values were assessed as the mean of five evenly distributed measurements across a 2 m $x$ 2 m plot (4 quadrants & 1 centre).

Table 1: List of input parameters for the radiative transfer model PROSAIL. We incorporated traits from (1) in-situ trait measurements and leaf sampling in the plots, (2) from structural measurements of canopy characteristics, and (3) from other sources. Site-specific ranges can be found in Tab. A.6. spr - spring, sum - summer, aut - autumn.

| Parameter | Description | Ranges | Source or equation |
|---|---|---|---|
| **(1) Leaf- and plant-based parameters** | | | |
| Cab ($\mu g/cm^2$) | Chlorophyll a & b content | spr 29 - 157<br>sum 26 - 167<br>aut 26 - 146 | SPAD conversion based on Markwell et al. (1995) + Standard Deviation derived from spectrophotometry (Ludwig et al. 2022), Cab $= 0.0893 * 10^{\text{SPAD}^{0.256}} + \text{SD}$ |
| Car ($\mu g/cm^2$) | Carotenoid content | spr 15 - 39<br>sum 10 - 41<br>aut 14 - 37 | Via linear regression from Cab content |
| Cbrown | Brown pigment content | 0 - 1 | Field observation: species-wise for brown (1) or green (0) individuals |
| Cw (cm) | Equivalent water thickness | spr 0.003 - 0.9<br>sum 0.001 - 0.5<br>aut 0.003 - 0.07 | $EWT[\frac{g}{m}] = \frac{LWC*LMA}{1-LWC}$<br>$EWT[cm] = \frac{1}{\frac{1000}{EWT[\frac{g}{cm}]}}$ |
| Cm ($g/cm^2$) | Leaf mass per area | spr 0.01 - 0.3<br>sum 0.001 - 0.15<br>aut 0.002 - 0.25 | Field sampling |
| **(2) Canopy-based parameters** | | | |
| LAI | Leaf area index | spr 0.3 - 5.0<br>sum 0.3 - 4.0<br>aut 0.5 - 5.0 | LiCor2200C |
| lidfa (°) | Mean Tilt Angle | spr 41 - 72<br>sum 30 - 71<br>aut 23 - 80 | LiCor2200C |
| **(3) Parameters from other sources** | | | |
| N | Structure parameter | Monocots & Dicots<br>spr 1.0-1.5 & 1.9-2.5<br>sum 1.4-1.7 & 1.6- 2.9<br>aut 1.5-1.7 & 1.6-2.9 | Boren et al. 2019 |
| rsoil | Background soil reflectance | reflectances from 0-1 | Spectrometry of site-specific soil samples (Fig. 10) |
| tts (°) | Solar zenith angle (°) | 34 - 58 | Calculated per site and season |
| tto (°) | observer zenith angle | 10 | Fixed |
| psi (°) | relative azimuth | 0 | Fixed |
| hspot | hotspot parameter | 0.01 | Fixed |

# Simulation experiment

## Simulated grassland communities

We used site- and species-specific field data from the vegetation surveys in order to generate spatially explicit two dimensional point pattern distributions that represent artificial grassland communities of different diversity levels (hereafter 'grassland simulations'). All grassland simulations were created within an observation window of 30 m $x$ 30 m. This base size allowed us to represent the same grassland simulation in different spatial resolutions that resemble the most commonly used sensor types for grassland diversity monitoring (Tab. 2).

We applied two different point distribution functions from the *spatstat*-package in order to create the points patterns (i.e. grassland simulations). In the simulations, each plant individual is represented by a single point and all points are distributed independently from each other. Different species are included as different point types and specific parameters allow to include species-specific point densities in the distribution functions. In order to control the effect of the background soil reflectance, population densities were fixed to the same point numbers in all simulations (4000 (BL and LA sites) and 1000 (LU site) individuals per $m^2$). We calculated this density based on the composition of a common agricultural seed-mixture for pastures with an herb content of 10% (BL and LA sites) and nutrient-poor grassland (LU site, Tab. A.4). This number is comparable to other studies (Weiner et al. 2001), however, literature on grassland community simulations as detailed as ours is sparse. In the following, we describe the four steps of the simulation procedure exemplary for a single site and season (Fig. 2).

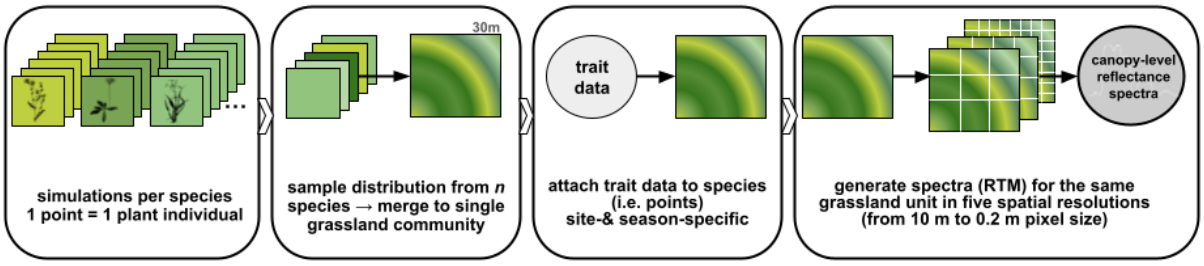


Figure 2: General workflow for point pattern distributions as basis for the grassland simulations. First, we use two point distribution functions to create 50 different point patterns per species. In this process, species-specific distribution patterns and cover fractions from field observations were considered. Second, point patterns are combined at different diversity levels to create the grassland simulations. Each diversity level is represented by 1000 grassland simulations with different species combinations. Third, trait values from field sampling are attached to the species individuals in the simulations. Forth, each simulated grassland is represented in five different spatial resolutions. Finally, pixel-wise canopy-level reflectance spectra are generated for the single grassland simulations in five spatial resolutions (from 10 m to 0.2 m pixel size).

First, we created point pattern distributions within the observation window for each single species that was recorded in the vegetation surveys. The observation window was set to 30 $x$ 30 area units. We further included the recorded species-specific cover fractions from all plots to include the observed variations in the simulations. An adjustment of the observation window allowed us to scale the number and density of points from the plot level up to the desired grassland simulation size of 30 m $x$ 30 m. Two types of point

pattern functions were applied: (1) a homogeneous Poisson point process (Kingman 1992) for species such as *Bromus specs.*, *Arrhenatherum spec.* or *Poa specs.* with a homogeneous distribution pattern across the study sites, and (2) a Matérn cluster process (Matérn 1960) for species such as *Nardus stricta* or bigger clusters (e.g. *Tanacetum vulgare*).

The Poisson point process is realised by the *rmpoispp*-function in *spatstat* (Baddeley et al. 2005). Here, point patterns are created based on the intensity function $\lambda(x, y, m)$. $\lambda$ is "the average number of points of type m per unit area near the location *(x, y)*" (ibid.). We parameterised $\lambda$ by incorporating a vector including the different cover fractions of each species as recorded in the 20 plots at the respective observation time. The Matérn cluster process (Matérn 1960) is realised by the *rMatClust*-function (Baddeley et al. 2005). This process includes the intensity factor $\kappa$ that describes the expected number of cluster centres per unit area. We parameterised $\kappa$ using the respective species' abundance probability across the whole field site that was recorded during the vegetation survey. The *scale* argument defines the radius of the cluster, we parameterised it by using the plot-wise cover fractions for the respective species. The argument $\mu$ allows defining the mean number of points per cluster and is set to a random number between 10 and 100 as the exact number of individuals per cluster is hard to define in the field. Every point is attributed with $x/y$ coordinates within the observation window. We created a total number of 50 independent point pattern distributions per species. Since the points are distributed randomly in each iteration, a reasonable variation between the point patterns is included in the simulations.

Second, we created 1000 grassland simulations for five different diversity levels ($n$ = 5, 10, 15, 20, 25 species, respectively) by random sampling of $n$ single distribution patterns from the before created point patterns to one combined grassland simulation containing $n$ species. 1000 ensure ample variations but are still computationally feasible. The random sampling included a probability vector based on the relative cover fractions to maintain the species ratios as recorded in the field. The sampling for one grassland simulation was repeated until the area was filled with the respective point numbers (BL & LA sites: 4000 points/ 1 area unit, LU site: 1000 points/ 1 area unit). Consequently, all grassland simulations for one site contain the same point numbers (i.e. plants) regardless of species numbers they contain. Third, we incorporated the collected in-situ trait data in the simulated grassland simulations. A coherent set of species-, site- and season-specific trait values was assigned to each point (i.e. plant individual) in the grassland simulations. The complete parameter list can be found in Tab. 1.

Forth, a set of five regular, quadratic grids was used to divide each simulated grassland simulation into virtual pixels. The grid width varied according to the spatial resolution of commonly used optical sensors in Earth observation (Tab. 2). The points were assigned to the pixels of a unit based on their $x$-/$y$-coordinates. By that, we obtained pixel-wise species- and trait information. Mean trait values were calculated per pixel and passed to the RTM in order to generate canopy-level reflectance spectra of the simulated grasslands in the respective spatial resolution. This enabled us to directly test and compare the effects of sensor induced scaling effects based on the exact same grassland community.

The same procedure was followed for all three field sites and for three seasons each (including the site-

and season-specific species inventories and trait data).

Table 2: Spatial resolutions chosen in accordance to commonly used sensor types. Each simulated grassland simulation is represented in these five spatial resolutions. The pixel counts refer to the basic unit of a 30 m $x$ 30 m tile in our simulations.

| **spatial resolution** (m $x$ m) | 10 $x$ 10 | 6 $x$ 6 | 3 $x$ 3 | 1 $x$ 1 | 0.2 $x$ 0.2 |
|---|---|---|---|---|---|
| **pixel counts** | 3 $x$ 3 | 5 $x$ 5 | 10 $x$ 10 | 30 $x$ 30 | 150 $x$ 150 |
| **sensor type** | Sentinel-2 | RapidEye | Planet, SPOT | IKONOS | Digital Orthophoto |

### Radiative Transfer Model PROSAIL and model parameterisation

RTMs are physical models that can be used to simulate and describe the interactions of sunlight with plant canopies and the underlying soil. They can be applied to study the effects of reflectance, absorption and scattering on the leaf-level (e.g. PROSPECT, Verhoef 1985; Verhoef, W 1984) and canopy-level (e.g. 4Sail, Verhoef et al. 2007) and help in understanding the light-plant interactions. PROSAIL is a two-dimensional RTM that combines the leaf- and canopy-level interactions (Jacquemoud, Stéphane and Verhoef, Wout and Baret, Frédéric and Bacour, Cédric and Zarco-Tejada, Pablo J and Asner, Gregory P and François, Christophe and Ustin, Susan L 2009). We applied the hemispherical stream of PROSAIL implemented in the *hsdar*-package (Lehnert et al. 2019) which uses a combination of Prospect-5B (Feret, JB and François, C and Asner, G and Gitelson, A and Martin, R and Bidel, L and Ustin, S and Le Maire, G and Jacquemoud, S 2008) and 4Sail to generate pixel-based reflectance spectra for the simulated grassland simulations on the canopy-level. To reduce the dimensionality of the data, we first performed a spectral resampling to 10 nm width using the *spectralResample*-function and removed the water bands (1340 - 1420 nm and 1800 - 1940 nm). The remaining hyperspectral data (188 bands) were kept across all spatial resolutions.

## Diversity metrics: spectral, taxonomic and functional diversity

Based on the species abundances and trait data, we calculated different indices for taxonomic diversity for every single grassland simulation using the *FD*-package (Laliberté et al. 2014). Previous studies led to ambiguous results regarding the strength of the relationship between spectral diversity and different taxonomic diversity indices (Badourdine et al. 2022; Fauvel et al. 2020; Oldeland et al. 2010; Wang et al. 2018b). Consequently, we tested the four most commonly used indices (Tab. 3): (1) species richness (SR), (2) Shannon's diversity index (H'), (3) Simpson's diversity index (D), and (4) Rao's quadratic entropy (Rao's Q). Shannon's and Simpson's diversity index both include the evenness and species richness of a plant community, whereas Shannon's Index is more sensitive to rare species. Due to the differences in units and trait value ranges, the data were scaled and centred before the calculation of Rao's Q.

Based on the 188 bands of the pixel-wise reflectance spectra, we calculated two spectral diversity indices for every grassland simulation in five different spatial resolutions, respectively: (1) the mean Euclidean

Table 3: Taxonomic and functional diversity indices used in this study, their description and source.

| Index | Short | Description | Source |
|---|---|---|---|
| Species Richness | SR | The species count in a given grassland simulation | – |
| Shannon's diversity index | H' | A measure of entropy that considers the species' proportions besides species numbers in the quantification of diversity | Magurran et al. 2010 |
| Simpson's diversity index | D | Describes the probability of selecting two different species from random sampling with replacement; sensitive to imbalanced species proportions | Simpson 1949 |
| Rao's quadratic entropy | Rao's Q | Includes the species abundances as well as the dissimilarities among the species in the multi-dimensional trait space | Botta-Dukát 2005 |

distance (mED, Rocchini, Duccio and Chiarucci, Alessandro and Loiselle, Steven A. 2004) as the mean values of pairwise mED between the pixels of one grassland simulation, and (2) Rao's Q which is the abundance-weighted sum of squared pairwise distances between wavelength reflectances (hereafter 'spectral Rao's Q', Rocchini, Duccio and Marcantonio, Matteo and Ricotta, Carlo 2017). We used the *FD*-package to calculate spectral Rao's Q from the first nine components after performing a PCA on the spectral data to reduce its dimensionality (Dahlin 2016). The reflectance data were scaled and centred beforehand. Finally, the correlations between the different taxonomic, functional and spectral diversity indices were tested using Person's correlation coefficient from linear correlation analyses (R, -1 to +1).

# 3 Results

The number of recorded species varied between field sites and seasons and ranged from 14 (LA site, nutrient poor) to 34 (LU, dry grassland, Tab. 5). Additionally, a multi-seasonal set of leaf samples was collected to provide species-, site- and season-specific traits for the grassland simulations that were passed to PROSAIL. An overview on the number of collected samples can be found in Tab. 5.

**Spectra across diversity levels and seasons**

The grassland simulations were based on in-situ trait measurements and coupled with RTMs to generate community specific reflectance patterns. The resulting spectra show typical spectral vegetation features and are comparable to spectral field measurements. In the region of the visible light (vis, 400 - 700 nm), the chlorophyll-peak is clearly expressed and shows slight changes across the seasons indicating minimal changes in chlorophyll concentrations (Fig. 3 & Fig. A.13). The red edge (750 nm) and NIR-plateau (700 - 1300 nm) are fully expressed in all sites and seasons. Changes in the NIR-plateau are apparent in the spectra from the BL and LU sites from spring to summer (Fig. 3 & Fig. A.13) indicating stressful

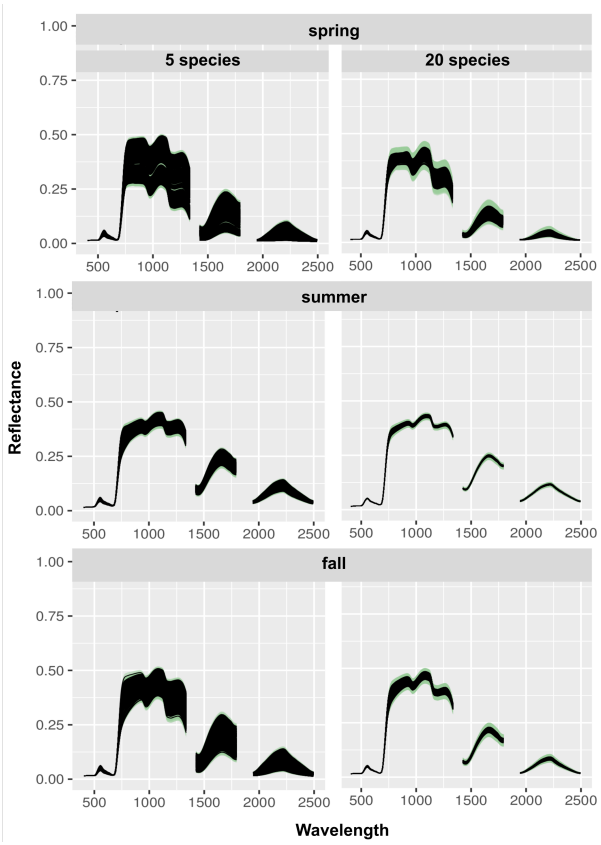


Figure 3: Median reflectance spectra of the 1000 simulated grassland communities for the lowest and highest species numbers in each season in the BL site. Black lines depict the median spectrum of a single grassland simulation in the finest spatial resolution, i.e. the median spectrum of the reflectance spectra of 22500 pixels in one simulated grassland simulation. Green areas show the upper and lower quartiles (75% and 25%) of the pixel-wise spectra from the single simulations. Exemplary for BL - Bad Lauchstädt (nutrient rich). The reader is referred to the supplementary for the remaining sites.

conditions around the time of sampling that can be related to heat or drought. Further, the spectra from the LU site (nutrient poor) show a less prominent red edge and NIR-plateau. The absence of a well-defined red edge and a less distinct NIR-plateau can be indicative of sparse vegetation or canopy gaps which is typical for dry grassland areas. In areas with lower vegetation density or gaps in the canopy, the reflectance signal may be influenced by a mixture of both vegetation and background reflectance (Fig. A.13). In the spectra from the LU site, the influence of the background soil reflectance caused by the lower population density in the simulations is clearly visible. The SWIR-region (1300 - 2500 nm) is affected by leaf water content and structure. Regarding spectra of the five species simulations, the variability in this region is particularly high if the influence of the soil reflectance is stronger (LU site, Fig. A.13).

### Links between taxonomic and functional diversity

We simulated grassland communities in different spatial resolutions and generated their spectral reflectances on the canopy level using RTMs in order to examine the spectral-to-species diversity relationship. According to the SVH, a strong link is expected. We used mED and Rao's Q to calculate spectral diversity. Although both metrics only show a weak correlation (Fig. 17), the overall patterns between the different indices for taxonomic, functional and spectral diversity are the same. In the following, we describe the results referring to mED as spectral diversity metric (see Fig. 18 for spectral Rao's Q).
The overall patterns resulting from the correlation analysis were inconsistent across the study sites and seasons. Only few variables showed the expected stable positive relationship, such as Shannon- and Simpson-Index since they are mathematically related to each other. Further, both species diversity indices were significantly correlated with species numbers ($p < 0.05$ for all sites and seasons, specific $R^2$-values are indicated in Fig. 5, Fig. A.14). Shannon's and Simpson's Index increased with increasing species number across all sites and seasons (Fig. 5 & A.14). In contrast, raw species numbers showed no or only in some cases weak to moderate correlations to functional trait diversity (FD, Fig. 4, Fig. 18). This is especially apparent for LU where mean Rao's Q values are almost stable across the five diversity levels and seasons (Fig. 5). Results from the linear regression indicate a significant relationship between FD and SR ($p < 0.05$ for all seasons) but also that a major part of the total variation in the data cannot be explained by the model ($R^2 < 0.05$ for all seasons).

### Links between spectral diversity, taxonomic and functional diversity

Results from our simulation experiments did not show a consistent correlation between raw species numbers and spectral diversity. This was the case for both mED and spectral Rao's Q (Fig. 18). The assumption of the SVH that higher species numbers result in higher spectral diversity was only met in one site and season ($BL_{spring}$, Fig. 4). In the BL site, the strength of the correlation increased towards

finer spatial resolutions (from $R_{10m}$ = 0.37 to $R_{0.2m}$ = 0.68, Fig. 4). In summer, R-values for the BL sites differed strongly between the five spatial resolutions and indicate a negative correlation towards the finest spatial resolution (from $R_{10m}$ = 0.01 to $R_{0.2m}$ = -0.5, Fig. 4). The opposite was the case for the same site in autumn (Fig. 6). Also regarding the other sites and seasons, correlations between raw species numbers and spectral diversity for different spatial resolutions were not stable. On the LA site, both strength and direction of the correlation changed across the seasons (Fig. 4). On the dry grassland site (LU site), results from the simulations indicate an inverse correlation between raw species numbers and spectral diversity on different spatial scales (Fig. 4). Moving from raw species numbers to abundance weighted diversity indices, the correlation analysis did not reveal a stable pattern. In some cases, the correlation between spectral diversity and Shannon's or Simpson's index was strongly pronounced and increased towards finer spatial resolutions (e.g. $BL_{spring}$, $R_{Shannon,\ 0.2m}$ = 0.72 and $LA_{summer,autumn}$, Fig. 4). However, this trend was highly variable across sites and seasons. For the LU site, R-values generally ranged around R = 0, indicating no correlation between Shannon- or Simpson index and spectral diversity across all spatial resolutions.

**Links across sites, seasons and spatial resolution**

Summarised for seasons and spatial resolutions, the relationship between species numbers and spectral diversity was weak and varied between sites as well as seasons (Fig. 7A). For the dry grassland site (LU site), R-values indicate a negative relation between species numbers and spectral diversity and show low variation across seasons and spatial resolutions. The opposite was the case for the BL site, where R-values vary substantially across the seasons and spatial resolutions and range from positive to negative R-values. However, the median $R_{BL} \approx 0$ indicates no correlation between the two variables in general. Correlations between the abundance-weighted Shannon-Index and spectral diversity were weak for all sites (median $R_{BL} = 0$ to median $R_{LA} = 0.25$, Fig. 7A). R-values from the three sites ranged between $R = -0.25 - 0.75$ across seasons and spatial resolutions and did not show a clear trend (Fig. 7A). With regard to functional diversity (Rao's Q), median R-values were positive and similar for all sites (median $R_{BL,LA,LU} = 0.2$, Fig. 7A), however, indicating a weak positive correlation with spectral diversity. Additionally, the variation of R-values across the seasons and spatial resolutions differed between the sites.

Considering single seasons, the strength and direction of the correlation between the different indices and spectral diversity was both index- and season-specific. Median R-values across all sites indicate a negative correlation between species numbers and spectral diversity for all seasons (Fig. 7B). Median R-values for correlations between Shannon-index and spectral diversity were low, indicating a weak relationship between the two variable (Fig. 7B). The same was true for Rao's Q, although the range of R-values across sites and spatial resolutions within one season were larger. In general, the ranges differed between the seasons and indices and did not show a clear pattern. For the number of species, results indicate a

large variation in R-values in spring which decreased towards autumn, i.e. correlations between species numbers and spectral diversity became more similar between sites and spatial resolution in autumn. Regarding functional diversity (Rao's Q), a contrary trend was observed.

With regard to the spatial resolution, the strength and direction of the correlation depended both on the considered metric and the spatial resolution itself. Median R-values for the correlation between species numbers and spectral diversity are stable around R = -0.25 (Fig. 7C). The variation in R-values for all sites and seasons increased towards the finest resolution. Median R-values indicate no correlation between Shannon-Index and spectral diversity at coarse resolutions (median $R_{10m-1m} \approx 0$, Fig. 7C) and a slight positive trend towards the finest resolution. For Rao's Q, results indicate an increase in the strength of the correlation with spectral diversity towards the finest resolution. Additionally, the variation of the R-values across sites and seasons is lowest for this index (Fig. 7C).

Regarding the relation between spectral diversity and spatial resolution in detail, results from the grassland simulations show a strong influence of the spatial resolution on the simulated spectral diversity. Across all sites and seasons, spectral diversity increases towards the finest spatial resolutions (Fig. 8).

# 4 Discussion

Using a simulation setup to generate large numbers of artificial grassland communities provides a scalable framework to robustly assess the theoretical background of the spectral-to-species diversity relationship. Based on multi-seasonal and site-specific field sampling, the simulated communities exhibit through the course of seasonal changes regarding both species composition and trait expression. This provides the unique opportunity to contextualise our findings with a direct link to the observed habitat itself. Our results underline the strong context dependency of the proposed relationship as both spatial scale and habitat type strongly influence the correlation between spectral and species diversity. The relationship between SR and FD mediates the species-to-spectral diversity relationship, however, this basic assumption of the SVH is not fulfilled in all plant communities. Further, seasonal effects are likely to be masked by the impact of site-specific management on local plant traits.

Based on our simulations, we cannot support the transferability of the SVH across habitat types. Our results rather reflect the context-dependency of the proposed relationship between different aspects of biodiversity and spectral diversity, showing positive correlations for single cases only. Recent literature has shown ambiguous results regarding the application of the SVH for plant diversity detection. Several studies based on single habitat types provide robust evidence for a positive correlation between spectral and species diversity (Badourdine et al. 2022; Rocchini et al. 2014; Rocchini, Duccio and Chiarucci, Alessandro and Loiselle, Steven A. 2004). However, other studies regarding a broader spatial extent covering different habitats reported unstable or negative relationships (Fassnacht et al. 2022; Schmidtlein et al. 2017), supporting the paradigm of habitat-dependency (Perrone et al. 2023). Considering the variety

and uniqueness of single habitat types, the observed inconsistencies among results do not come as a surprise. We included intraspecific trait variability (ITV) across sites and seasons to account for this variety, generating RTM based canopy reflectance spectra. This separates our experimental design from studies using random samples out of predefined trait ranges. Using trait ranges might be appropriate for agricultural study sites with more or less controlled conditions where community structure and environmental settings are homogeneous. Here, one can assume lower intraspecific trait variability (ITV) (Herrick et al. 2021). This assumption does not account for semi-natural grasslands: a global meta-analysis by Siefert et al. (2015) has shown that ITV accounts for up to 25% of the total within-community trait variance. Consequently, using individual-based trait values allowed us to account for ITV to some degree and mimic spectral responses more close to reality. Within a plant community, species vary in abundance and cover fractions. This introduces another dimension of heterogeneity into the habitat. Our simulations were set up in a way that maintained the proportions of the single species as they were recorded in the field to ensure reasonable cover fractions in the grassland communities. As a consequence, dominant species from the respective field sites remain dominant in the simulations along the diversity gradient and are weighted more heavily in the calculation of FD. This is reflected in the low correlations between FD and SR (Tab. A.7). The inconsistent relationship between SR and FD leads us away from the notion of spectral diversity as measure for SR. The identity of single species in a plant community is not the most relevant parameter with regard to its canopy reflectance. Similar as in the concept of plant functional types (PFT), we can assume that the optical contribution of species is more important than their identity. The concept of PFTs can help to group plant species according to their responses to the environment and their effects on ecosystem functioning (Díaz, Sandra and Cabido, Marcelo 2001). In our study, we focused on trait measurements from individual species to calculate FD. However, the species converge in only a few PFTs which is further increased through the skewed abundances of single species. Our results show that variations in FD within the same diversity level were larger than the variation of FD between the different diversity levels. This indicates the occurrence of a limited set of dominant species with characteristic optical traits across the simulations of different diversity levels. It is likely that the same dominant species (or PFTs) are the main contributors to FD for the individual sites, regardless of the simulated SR. Variations in vegetation cover have been reported to be a dominant driver of spectral diversity in grasslands (Hauser et al. 2021). In our simulations, we minimised the influence of soil, environment and textures to particularly shed light on the effects of optical traits and canopy structure across sites and seasons. Earlier versions of the grassland simulations with low population densities resulted in large proportions of bare soil pixels in fine spatial resolutions (3 m and smaller, results not shown) and did not allow drawing conclusions on the importance of optical plant traits on spectral diversity. Therefore, population densities were estimated based on seed mixtures (4000 individuals / $m^2$ for the BL and LA sites). Only for the dry grassland site (LU site) we chose a lower population density to represent the natural conditions of this specific habitat type appropriately (1000 individuals / $m^2$). In this case, the simulations reflect the strong impact of background soil reflectance which can be typical

for dry grasslands and hampers diversity estimations based on RS data for these habitats. Less dense vegetation inevitably leads to a stronger impact of the background soil reflectance (Fig. A.13), textures and environmental heterogeneity on the spectral signal. Setting this high content of spectral information in relation to sparse vegetation can lead to an inverse spectral-to-species diversity relationship as reported here and in recent studies (Fassnacht et al. 2022; Hauser et al. 2021; Rossi et al. 2022). Comparing our results (inconsistent relationship between SR and spectral diversity) to previous studies, we can assume that not trait and canopy features, but excluded factors, such as texture and environmental features, dominate spectral diversity. The role of background soil reflectance allows various interpretations, as results from dry grassland sites have shown. However, our results underline the context-dependency of the proposed relationship (see also Perrone et al. 2023; Schmidtlein et al. 2017). Finally, we need to consider that, compared to the global spectrum of grassland types, the grasslands chosen as reference in our study are rather homogeneous in structure and vegetation composition (all temperate grassland from the same latitude). However, differences in the spectral-to-species diversity responses in our simulations are already heavily pronounced between study sites. Different species communities and dynamics lead to complex patterns of spectral diversity in both space and time (Rossi et al. 2021). Interestingly, our results do not suggest substantial differences in the spectral-to-species diversity relationship between seasons. This can be explained by the site-specific dynamics and management which influence the vegetation structure and species compositions and are therefore captured by our trait sampling. We collected data from study sites with different management regimes: The LA site (nutrient-poor) was mowed in early summer, consequently the plant community and its related traits from the summer sampling rather resemble a typical spring community. The LU site (dry grassland) was occasionally grazed by sheep which partially disturbed the growth of distinct herbaceous species and led to a homogeneous canopy height. Only the BL site (nutrient-rich) remained undisturbed throughout the whole vegetation season. However, the zero-impact management regime caused an accumulation of dead biomass, i.e. increasing the percentage of photosynthetically inactive vegetation in the plots. These different dynamics represent a part of the complex variety of confounding factors in spectral-to-species diversity relationships that occur in "real-world" scenarios and influence this relationship over time. Although the time point of data acquisition is crucial for a more reliable diversity detection from RS data (Thornley et al. 2022), our results clearly show that results can still be misleading if management is not taken into account and support a major flaw of the SVH for SR detection (Fassnacht et al. 2022). In the context of utilising the spectral variation approach, it may be prudent to reconsider the exclusive pursuit of SR as an ecological target. Instead, a more comprehensive understanding of ecosystem dynamics may be attained by concurrently considering both the spatial and temporal dimensions of spectral diversity. In this regard, Rossi et al. (2021) have presented promising findings that exemplify this integrated approach. The mediating role of spatial resolution on the strength of the spectral-to-species diversity relationship has been repeatedly reported in recent studies (e.g. Fassnacht et al. 2022; Rossi et al. 2022; Thornley et al. 2023). Based on findings from an experimental grassland site, Wang et al. (2018b) showed that the spectral-to-species

relationship breaks down from pixel sizes of 10 cm x 10 cm and larger. The same pattern is reflected in our results which show an increasing strength of the correlation between FD and spectral diversity towards the finer spatial resolutions (1 m, 0.2 m, Fig. 7). However, our results cannot confirm that spectral diversity at finer spatial resolutions is directly related to higher FD as the correlation across sites and seasons is weak (Tab. A.7). On the contrary, spectral diversity increases with finer spatial resolutions more significantly than with increasing FD (Fig. 8). The spectral signal obtained from a pixel is composed by all optical traits of the species present within this pixel and the larger the difference between the pixel size and the size of the plant individual, the more mixed is the spectral signal. The mismatch of this ratio is heavily pronounced in grasslands and leads to a strong spectral mixture. In general, a relationship between spectral diversity and SR is not to be expected at spatial resolutions that exceed the size of a plant individual (Fassnacht et al. 2022; Thornley et al. 2022). To overcome the limitations of SR, the use of abundance-weighted diversity metrics has been recommended by different authors (Heumann et al. 2015; Oldeland et al. 2010; Wang et al. 2018a). Based on our simulations, the application of the Simpson or Shannon index did not lead to stronger correlations or more consistent results across sites, seasons or spatial resolutions. It can be assumed that the spatial arrangement of a plant community has a strong impact on the detected spectral signal. Different growth types (patchy vs. homogeneous) and heterogeneous plant cover fractions across an area can increase spectral diversity independently from the SR within the area. Rare species or species with low cover fractions are likely to be underrepresented in the spectral signature. Considering the complex three dimensional structure of the stands, this effect would be even more heavily pronounced as their optical traits do not contribute to the spectral signal, which is a function of exposure towards the sensor. This fundamental weakness of the SVH has already been pointed out by Fassnacht et al. (2022) and our results indicate that this may hold true: even if regarded for an 'ideal' scenario including only canopy-reflectance, spectral diversity cannot reflect SR or FD as long as species are not equally distributed (spatially and abundance-wise) within the regarded area. Unfortunately, species are usually not distributed homogeneously in natural ecosystems and our simulations clearly show this flaw that hinders a reliable universal application of the SVH across ecosystem types. The same fundamental limitations occur in the context of the so-called spectral species concept (Féret, JB and Asner, G 2014). This concept likewise assumes that species feature unique sets of optical traits that lead to distinct spectral differences. However, the actual size of the species in relation to the pixel size as well as their spectral and trait-based uniqueness determine whether this assumption actually holds true (Rocchini et al. 2022). These complex dependencies can also explain the variable relationships observed in our study. Interestingly, the choice of spectral diversity index did not change the outcome of the correlation analysis and the variability of the spectral-to-species diversity relationship is equally represented by mED and spectral Rao's Q (Fig. 4, Fig. 18). In comparison to mED, the calculation of spectral Rao's Q requires much higher computational efforts while potentially delivering similar informative value (see also Perrone et al. 2023). Although of high interest, it is beyond the scope of this study to analyse the performance of different spectral diversity indices. However, the introduced

simulation framework provides the basis for further research on this topic.

## Challenges and limitations

Only a few studies tried to tackle the spectral-to-species diversity relationship based on plant community simulations. Badourdine et al. (2022) applied a restricted modelling process by creating rain forest tree populations based on a stratified random sampling of spectral data acquired from imaging spectroscopy. Although presenting promising results for forest diversity monitoring, the authors state that their study design leaves open questions with regard to the actual drivers behind the positive relationship. Using spectral data that cannot be related to in-situ measurements does not provide the needed information on trait combinations, canopy structure and community assembly underlying the observed spectral diversity. Pacheco-Labrador et al. (2022) approached the SVH by creating artificial plant communities based on species-specific trait data from trait databases fed into RTMs to generate spectral data. This design allowed them to generate a large number of species-specific spectra that could be used for the sampling of plant communities. Again, this study presented a positive spectral-to-species diversity relationship, however, spatial effects and the context-dependency of ecosystem types cannot be considered under this setup. Following up on these promising studies, we addressed the research gap by creating spatially explicit grassland community simulations. In our simulations, the spectral signal is highly influenced by the species/ trait distribution, species cover fractions and canopy structural parameters that are based on site- and season-specific in-situ measurements. It should be noted that our simulations represent an 'ideal' state of canopy-reflectance: they do not include parameters such as dead biomass and assume ideal illumination conditions. The simulations were designed in order to unravel the spectral-to-species diversity relationship caused by optical leaf traits only, i.e. to test the theoretical background of the SVH which is mainly the interactions between spectral, species, and functional trait diversity. Determining the number of plant individuals per unit area posed a challenge in configuring the simulation. Population densities vary across habitats and regions, and precise figures are limited in the relevant literature. While not the optimal approach, we derived population densities from agricultural seed mixtures. This method enabled us to establish an upper limit for plants in the simulated observation area, ensuring sufficiently high cover fractions to minimize strong background reflectance. Simultaneously, it maintained the population density at a level conducive to the realistic coexistence of plants under plausible conditions. For some delicate species (e.g. *N. stricta, A. serpyllifolium*), SPAD measurements are impossible or potentially not robust. This might introduce bias in the generated canopy-level reflectances as the retrieval of chlorophyll content for the RTMs is not ideal. The use of the SPAD instrument is not ideal for semi-natural grasslands (Ludwig et al. 2022). However, including the variation of SPAD vs. chemical measurements in the chlorophyll calculations is, for now, an appropriate measure to tackle the insensitivity of SPAD measurements for community means of chlorophyll contents. Considering the simulated spectra, our models delivered spectral reflectance patterns for grasslands of different habitats and diversity levels that

are comparable to spectral field measurements. Interestingly, the variance between the median spectra of the single grassland simulations is highest for the lowest diversity levels (Fig. 1). This is very likely caused by the limited species pool that we used as the basis for the grassland simulations. As an example: Based on a species pool of 20 species that we randomly drew from (without replacement), grasslands consisting of 15 species will be more similar to each other than grasslands with only five species drawn from the same species pool. This similarity in species composition within the same diversity level and, consequently, optical traits, is reflected in the spectral signal of the grassland simulations. Two parameters associated with changes in spectral diversity have not been included in our simulations: flowers and differences in life forms. The presence of flowers is timely limited and coupled with a decrease of chlorophyll levels, thereby altering the reflectance spectrum of a plant community on short time scales (Shen et al. 2009). Colour pigments of non-greenish flowers are associated with changes in the VIS and NIR regions of the electromagnetic spectrum of light. They increase reflection in the VIS region and cause lower reflectance in the NIR and MIR regions (Landmann et al. 2019). By that, flowers add up on spectral information while SR is not increasing which might lead to an overestimation of SR by additionally increasing spectral diversity. They further argue that flowers drive spectral diversity by the spatial aggregation of flowers within an area (patchiness) and asynchronous flowering patterns (Almeida-Neto et al. 2004). Both cases would result in an overestimation of SR based on spectral diversity. In contrast to this assumption are recent results which indicate that the retrieval of plant traits from spectral data is hindered in the presence of increasing flower proportions (Schiefer et al. 2021). A decreased predictive power of traits from RS data inevitably leads to inaccurate estimates of FD which weakens the application potential of the SVH. Additionally, grassland communities are shaped by compositions of different life forms that show distinct adaptations to the environmental conditions of their habitat (Raunkiaer et al. 1934). We did not include this concept in our simulations, however, it can be assumed that the presence of species with an increased proportion of non-green material (bark, dead biomass) additionally influences spectral diversity. *Cbrown* has a strong impact on spectral diversity (Torresani et al. 2021) . Although they relate this effect mainly to changes in leaf pigments, the same accounts for the bark of woody species (e.g. dwarf shrubs such as *C. vulgaris*). Further research will be necessary to investigate the role of flowers and different life forms in the spectral-to-species diversity relationship. With the presented simulation setup, we created a suitable tool to address these research gaps in future work.

## Conclusions & Outlook

According to the SVH, a positive relationship between spectral and species diversity in RS images is assumed. We present a detailed assessment of the SVH based on grassland simulations that were built on site- and season-specific vegetation surveys and in-situ trait measurements. Coupled with RTMs, our approach allowed an in-depth analysis of the theoretical background of the proposed relationships regarding different habitats, seasons and spatial resolutions. Our simulation design enabled us to bring an ecological context into our findings. In general, the universal applicability of the SVH for biodiversity

monitoring across seasons, sensors and ecosystems is lacking proof. Based on 45000 grassland simulations in five different spatial resolutions each, we could show that the spectral-to-species diversity is not stable across seasons and habitat types. Further, spectral diversity is mainly driven by the spatial resolution (i.e. pixel size) of the image and not by SR or FD per se. Moreover, we can assume that FD, which is an important driver of the spectral signature of a plant community, is not directly linked to the number of present species in an image. Our results clearly underline the context-dependency of the SVH and we argue that, although of promising value for distinct ecosystems, it is not universally applicable (Fig. 9).

The presented framework provides ample opportunities to further assess the spectral-to-species relationship regarding various aspects. By maintaining the hyperspectral resolution across all investigated spatial resolutions, our simulations provide the basis to assess the potential of future sensors that will possibly provide remote sensing data of finer spectral resolution than current missions. To analyse the effect of flower coverage across different spatial scales would be easily possible by including different flower spectra in the simulations. The same is true for different PFTs. Taking high computational resources into account, the simulations can be adjusted to finer spatial resolutions. Although of interest, it is beyond the scope of this study to test the impact of different measures for spectral diversity on the spectral-to-species relationship. However, this issue is definitely an aim of further research. We recognise that our study again brings focus to temperate grasslands only, as has been negatively pointed out as a shortfall in grassland monitoring studies (Thornley et al. 2023). However, the presented framework allows us to incorporate data from other suitable study sites which we warmly encourage. To conclude, the relevant question about what facet of diversity is the target objective of a study must be carefully considered when interpreting results from spectral diversity assessments. The importance of understanding ecological concepts behind SR, species diversity and FD is a crucial prerequisite for reliable biodiversity assessments. Further, driving factors behind spectral diversity in RS images can be of many origins and are hard to disentangle without detailed in-situ measurements and a clear understanding of the surveyed habitat. Therefore, the further development of urgently needed tools for grassland diversity monitoring will involve the collaboration of RS experts and ecologists.

# 5 Acknowledgements

This study was financed by the Helmholtz-Centre for Environmental Research (UFZ) as part of the *MoDEV*-PhD college - "Towards novel Model-Data fusion for understanding Environmental Variability in space and time from high-resolution remote sensing" (https://www.ufz.de/index.php?en=48638). The scientific results have (in part) been computed at the High-Performance Computing (HPC) Cluster EVE, a joint effort of both the Helmholtz Centre for Environmental Research - UFZ (http://www.ufz.de/) and the German Centre for Integrative Biodiversity Research (iDiv) Halle-Jena-Leipzig (http://www.idiv-biodiversity.de/). A.L. thanks Michael Seidel for the introduction to spectral soil measurements, Reimund Goss and Severin Sasso for supporting the spectrophotometric measurements, Khalil Teber and

Sebastian Preidl for occasional coding support, and all reviewers for their constructive feedback on earlier versions of the manuscript.

# 6 Author Contributions

**A.L.**: Investigation, Methodology, Software, Formal Analysis, Data Curation, Writing - Original Draft, Visualisation, Project administration; **D.D.**: Methodology, Software, Writing - Review & Editing, Supervision, Funding acquisition, Project administration; **H.F.**: Conceptualisation, Methodology, Writing - Review & Editing, Supervision, Funding acquisition, Project administration

# 7 Appendix

### Calculation of population density and point patterns

Under consideration of the sowing quantity per area and the species-specific weight of 1000 seeds, we derived an appropriate estimation of plant individual numbers. An exemplary calculation is presented in table A.4. Details on the two different used point pattern distribution types can be found in figure A.12.

Table 4: Proportion of species (in %) in a seed mix (40 kg/ ha) for a universal pasture grassland with 10% herb content. Including the weight of 1000 seeds per species ("Tausendkorngewicht", tkg) and the final number of seeds per $m^2$. The description of the seed mix was taken from *Camena-Samen* (see https://camena-samen.com/gruenlandmischungen/ for further details).

| species | % | tkg (g) | seeds per gramm | in mix (in g) | seeds in mix per ha | seeds per $m^2$ |
|---|---|---|---|---|---|---|
| *Lolium perenne* | 34.90 | 1.30 | 769.23 | 14000.00 | 10769230.77 | 1076.92 |
| *Bromus spec.* | 8.00 | 4.00 | 250.00 | 3200.00 | 800000.00 | 80.00 |
| *Festuca spec.* | 29.90 | 2.00 | 500.00 | 12000.00 | 6000000.00 | 600.00 |
| *Anthriscus sylvestris* | 0.60 | 3.50 | 285.71 | 240.00 | 68571.43 | 6.86 |
| *Bellis perennis* | 0.20 | 0.10 | 10000.00 | 80.00 | 800000.00 | 80.00 |
| *Cirsium arvense* | 0.20 | 1.10 | 909.09 | 80.00 | 72727.27 | 7.27 |
| *Plantago lanceolata* | 2.20 | 2.00 | 500.00 | 880.00 | 440000.00 | 44.00 |
| *Stellaria media* | 0.60 | 0.40 | 2500.00 | 240.00 | 600000.00 | 60.00 |
| *Centaurea jacea* | 0.50 | 1.20 | 833.33 | 200.00 | 166666.67 | 16.67 |
| *Trifolium repens* | 8.00 | 0.65 | 1538.46 | 3200.00 | 4923076.92 | 492.31 |
| *Phleum pratense* | 15.00 | 0.40 | 2500.00 | 6000.00 | 15000000.00 | 1500.00 |
| Total | - | - | - | - | - | 3964 |

### Details on PROSAIL parameterisation

We used pixel-based trait means as input variables for each grassland unit (Table 1). Based on these parameters, we generated pixel-wise reflectance spectra for every grassland unit in its finest resolution (150 x 150 pixels). We then aggregated the reflectance spectra step wise towards the coarser resolutions by calculating the mean reflectance values from all spectra in the aggregated pixels. Consequently, we gained

Table 5: Number of recorded species (SR) and collected trait samples (nb Samp) from field campaigns per site and season.

| Site | Season | SR | nb Samp |
|---|---|---|---|
| BL | spring | 21 | 257 |
| | summer | 28 | 177 |
| | autumn | 23 | 187 |
| LA | spring | 15 | 137 |
| | summer | 17 | 121 |
| | autumn | 14 | 125 |
| LU | spring | 31 | 155 |
| | summer | 31 | 139 |
| | autumn | 34 | 176 |

a set of five spectral libraries for each grassland unit containing the respective number of spectra according to the number of pixels in the respective spatial resolution: From 22.500 spectra in the finest resolution (150 x 150 pixels) to nine spectra in the coarsest resolution (3 x 3 pixels). The same procedure was followed for all simulated grassland units from all diversity levels, sites and seasons. Some input parameters were, however, not easily measurable on the plants. They refer to specific plant characteristics which can often only be obtained with complex laboratory analysis. The structure parameter $N$, for example, is an unit less value that refers to the mesophyll structure of leaves based on a simple plate model (Jacquemoud, Stéphane and Verhoef, Wout and Baret, Frédéric and Bacour, Cédric and Zarco-Tejada, Pablo J and Asner, Gregory P and François, Christophe and Ustin, Susan L 2009). As monocotyledon and dicotyledon plants show different structural developments of their leaves, the $N$-value is often different for both of these classes. Monocotyledons are associated with a less complex mesophyll structure and, thus, fewer layers and receive smaller $N$-values than dicotyledons. Also the seasonal development and age of the leaves has a strong impact on their structure. Therefore, we chose to seasonally adjust $N$-values accordingly to both monocotyledons and dicotyledons. We chose N-values from the literature that are based on leaf-level inversions of the RTM PROSPECT for four different plant species (1 dicotyledon, 3 monocotyledon) at three different time points of the growing period (Boren et al. 2019). They provide so far the most reliable record of $N$-values. According to the season and class affiliation, a random value within the range of the given $N$-value was assigned to each species in the simulated community (Table 1). We further included background soil reflectance from site-specific spectral soil reflectance measurements as input variable for *rsoil*. If pixels remained free of points (i.e. plant individuals) they were filled with the site-specific bare soil reflectance spectrum. This was mainly the case for very high spatial resolutions (1 m x 1 m and 0.2 m x 0.2 m).

Table 6: Ranges of leaf traits, pigments and structural canopy parameters from field measurements per site and season. Cab: chlorophyll a & b content, Car: carotenoid content, Cw: Equivalent water thickness, Cm: leaf mass per area, LAI: Leaf Area Index, MTA: Mean Tilt Angle.

| Site | Season | Cab (mg/cm$^2$) | Car (µg/cm$^2$) | Cw (cm) | Cm (g/cm$^2$) | LAI | MTA (°) |
|---|---|---|---|---|---|---|---|
| BL | spring | 33-157 | 15-39 | 0.009-0.9 | 0.001-0.33 | 1.2-5 | 41-72 |
| | summer | 26-167 | 10-41 | 0.007-0.5 | 0.003-0.04 | 1-3 | 38-71 |
| | autumn | 27-146 | 14-37 | 0.003-0.07 | 0.001-0.04 | 1.4-4.7 | 23-63 |
| LA | spring | 29-85 | 15-25 | 0.003-0.07 | 0.001-0.04 | 3-5.8 | 40-62 |
| | summer | 27-81 | 14-24 | 0.007-0.09 | 0.002-0.03 | 1.2-4.1 | 39-67 |
| | autumn | 35-77 | 16-24 | 0.007-0.06 | 0.002-0.04 | 1.5-5 | 42-60 |
| LU | spring | 31-95 | 15-27 | 0.003-0.04 | 0.002-0.01 | 1.3-2.8 | 43-66 |
| | summer | 30-92 | 14-26 | 0.001-0.4 | 0.001-0.15 | 1.3-2.7 | 30-60 |
| | autumn | 26-102 | 14-29 | 0.008-0.25 | 0.003-0.2 | 1.4-3.1 | 35-80 |

742

Table 7: Results for different coefficients (from the linear regression models between different variables per site and season. All variables were calculated based on the grassland simulations. SR - species richness. Site codes: BL - Bad Lauchstädt (nutrient-rich), LA - Luppeaue (nutrient-poor), LU - Lunzberge (dry grassland). Significance levels (p-value, significance of correlation): 0 '***' 0.001 '**' 0.01 '*' 0.05 '.' 0.1 ' ' 1.

| Site | Coeff | Spring | Summer | Autumn |
|---|---|---|---|---|
| (1) lm(Shannon ~ SR) | | | | |
| BL | p | < 0.05 | < 0.05 | < 0.05 |
| | $R^2$ | 0.07 | 0.09 | 0.05 |
| LA | p | < 0.05 | < 0.05 | < 0.05 |
| | $R^2$ | 0.03 | 0.07 | 0.75 |
| LU | p | < 0.05 | < 0.05 | < 0.05 |
| | $R^2$ | 0.03 | 0.14 | 0.06 |
| (2) lm(Simpson ~ SR) | | | | |
| BL | p | < 0.05 | < 0.05 | < 0.05 |
| | $R^2$ | 0.64 | 0.39 | 0.71 |
| LA | p | < 0.05 | < 0.05 | < 0.05 |
| | $R^2$ | 0.19 | 0.13 | 0.21 |
| LU | p | < 0.05 | < 0.05 | < 0.05 |
| | $R^2$ | 0.38 | 0.50 | 0.09 |
| (3) lm(Rao's Q ~ SR) | | | | |
| BL | p | < 0.05 | < 0.05 | < 0.05 |
| | $R^2$ | 0.02 | 0.01 | 0.06 |
| LA | p | < 0.05 | < 0.05 | < 0.05 |
| | $R^2$ | 0.09 | 0.08 | 0.02 |
| LU | p | < 0.05 | < 0.05 | < 0.05 |
| | $R^2$ | 0.04 | < 0.01 | 0.02 |
| (4) lm($mED_{0.2m}$ ~ SR) | | | | |
| BL | p | < 0.05 | < 0.05 | < 0.05 |
| | $R^2$ | 0.47 | 0.26 | 0.01 |
| LA | p | < 0.05 | < 0.05 | < 0.05 |
| | $R^2$ | 0.13 | < 0.01 | < 0.01 |
| LU | p | < 0.05 | < 0.05 | < 0.05 |
| | $R^2$ | 0.14 | 0.13 | 0.12 |
| (5) lm($mED_{0.2m}$ ~ Rao's Q) | | | | |
| BL | p | < 0.05 | < 0.05 | < 0.05 |
| | $R^2$ | 0.07 | 0.09 | 0.05 |
| LA | p | < 0.05 | < 0.05 | < 0.05 |
| | $R^2$ | 0.03 | 0.07 | 0.75 |
| LU | p | < 0.05 | < 0.05 | < 0.05 |
| | $R^2$ | 0.03 | 0.14 | 0.06 |

# References


Almeida-Neto, Mário and Thomas M Lewinsohn (2004). "Small-scale spatial autocorrelation and the interpretation of relationships between phenological parameters". In: *Journal of Vegetation Science* 15.4, pp. 561–568.

Asner, Gregory P. (1998). "Biophysical and Biochemical Sources of Variability in Canopy Reflectance". In: *Remote Sensing of Environment* 64.3, pp. 234–253. ISSN: 0034-4257. DOI: https://doi.org/10.

1016/S0034-4257(98)00014-5. URL: https://www.sciencedirect.com/science/article/pii/S0034425798000145.

Baddeley, Adrian and Rolf Turner (2005). "spatstat: An R Package for Analyzing Spatial Point Patterns". In: *Journal of Statistical Software* 12, pp. 1–42. URL: https://www.jstatsoft.org/v12/i06/.

Badourdine, Colette, Jean-Baptiste Féret, Raphaël Pélissier, and Grégoire Vincent (2022). "Exploring the link between spectral variance and upper canopy taxonomic diversity in a tropical forest: influence of spectral processing and feature selection". In: *Remote Sensing in Ecology and Conservation*.

Boren, Erik J, Luigi Boschetti, and Dan M Johnson (2019). "Characterizing the variability of the structure parameter in the PROSPECT leaf optical properties model". In: *Remote Sensing* 11.10, p. 1236.

Botta-Dukát, Zoltán (2005). "Rao's quadratic entropy as a measure of functional diversity based on multiple traits". In: *Journal of vegetation science* 16.5, pp. 533–540.

Burg, Sarah, Christian Rixen, Veronika Stöckli, and Sonja Wipf (2015). "Observation bias and its causes in botanical surveys on high-alpine summits". In: *Journal of Vegetation Science* 26.1, pp. 191–200. DOI: https://doi.org/10.1111/jvs.12211. eprint: https://onlinelibrary.wiley.com/doi/pdf/10.1111/jvs.12211. URL: https://onlinelibrary.wiley.com/doi/abs/10.1111/jvs.12211.

Cardinale, Bradley J et al. (2012). "Biodiversity loss and its impact on humanity". In: *Nature* 486.7401, pp. 59–67.

Cavender-Bares, Jeannine, John A Gamon, Sarah E Hobbie, Michael D Madritch, José Eduardo Meireles, Anna K Schweiger, and Philip A Townsend (2017). "Harnessing plant spectra to integrate the biodiversity sciences across biological and spatial scales". In: *American Journal of Botany* 104.7, pp. 966–969.

Dahlin, Kyla Marie (2016). "Spectral diversity area relationships for assessing biodiversity in a wildland–agriculture matrix". In: *Ecological applications* 26.8, pp. 2758–2768.

de Bello, Francesco et al. (2021). "Functional trait effects on ecosystem stability: assembling the jigsaw puzzle". In: *Trends in Ecology & Evolution* 36.9, pp. 822–836.

Díaz, S. et al. (2019). "The global assessment report on biodiversity and ecosystem services: Summary for policymakers of the global assessment report on biodiversity and ecosystem services". In: *Intergovernmental Science-Policy Platform on Biodiversit and Ecosystem Services*.

Díaz, Sandra and Cabido, Marcelo (2001). "Vive la différence: plant functional diversity matters to ecosystem processes". In: *Trends in ecology & evolution* 16.11, pp. 646–655.

Fassnacht, Fabian Ewald, Jana Müllerová, Luisa Conti, Marco Malavasi, and Sebastian Schmidtlein (2022). "About the link between biodiversity and spectral variation". In: *Applied Vegetation Science* 25.1, e12643.

Fauvel, Mathieu, Mailys Lopes, Titouan Dubo, Justine Rivers-Moore, Pierre-Louis Frison, Nicolas Gross, and Annie Ouin (2020). "Prediction of plant diversity in grasslands using Sentinel-1 and -2 satellite image time series". In: *Remote Sensing of Environment* 237, p. 111536. ISSN: 0034-4257. DOI: https:

//doi.org/10.1016/j.rse.2019.111536. URL: https://www.sciencedirect.com/science/article/pii/S0034425719305553.

Feret, JB and F de Boissieu (2023). *prosail: PROSAIL leaf and canopy radiative transfer model and inversion routines*. R package version 1.2.3. URL: https://gitlab.com/jbferet/prosail.

Féret, JB and Asner, G (2014). "Mapping tropical forest canopy diversity using high-fidelity imaging spectroscopy". In: *Ecological Applications* 24.6, pp. 1289–1296. DOI: doi.org/10.1890/13-1824.1. eprint: https://esajournals.onlinelibrary.wiley.com/doi/pdf/10.1890/13-1824.1. URL: https://esajournals.onlinelibrary.wiley.com/doi/abs/10.1890/13-1824.1.

Feret, JB and François, C and Asner, G and Gitelson, A and Martin, R and Bidel, L and Ustin, S and Le Maire, G and Jacquemoud, S (2008). "PROSPECT-4 and 5: Advances in the leaf optical properties model separating photosynthetic pigments". In: *Remote sensing of environment* 112.6, pp. 3030–3043.

Gholizadeh, Hamed, John A Gamon, Arthur I Zygielbaum, Ran Wang, Anna K Schweiger, and Jeannine Cavender-Bares (2018). "Remote sensing of biodiversity: Soil correction and data dimension reduction methods improve assessment of $\alpha$-diversity (species richness) in prairie ecosystems". In: *Remote Sensing of Environment* 206, pp. 240–253.

Gibson, DJ (2009). *Grasses and grassland ecology*. Oxford University Press.

Hall, Karin, Triin Reitalu, Martin T Sykes, and Honor C Prentice (2012). "Spectral heterogeneity of QuickBird satellite data is related to fine-scale plant species spatial turnover in semi-natural grasslands". In: *Applied Vegetation Science* 15.1, pp. 145–157.

Hauser, Leon T, Joris Timmermans, Niels van der Windt, Ângelo F Sil, Nuno César de Sá, Nadejda A Soudzilovskaia, and Peter M van Bodegom (2021). "Explaining discrepancies between spectral and in-situ plant diversity in multispectral satellite earth observation". In: *Remote Sensing of Environment* 265, p. 112684.

Hautier, Yann, David Tilman, Forest Isbell, Eric W. Seabloom, Elizabeth T. Borer, and Peter B. Reich (2015). "Anthropogenic environmental changes affect ecosystem stability via biodiversity". In: *Science* 348.6232, pp. 336–340. DOI: 10.1126/science.aaa1788. eprint: https://www.science.org/doi/pdf/10.1126/science.aaa1788. URL: https://www.science.org/doi/abs/10.1126/science.aaa1788.

Herrick, Etienne and Jennifer Blesh (2021). "Intraspecific trait variation improves understanding and management of cover crop outcomes". In: *Ecosphere* 12.11, e03817. DOI: https://doi.org/10.1002/ecs2.3817. eprint: https://esajournals.onlinelibrary.wiley.com/doi/pdf/10.1002/ecs2.3817. URL: https://esajournals.onlinelibrary.wiley.com/doi/abs/10.1002/ecs2.3817.

Heumann, Benjamin W, Rachel A Hackett, and Anna K Monfils (2015). "Testing the spectral diversity hypothesis using spectroscopy data in a simulated wetland community". In: *Ecological Informatics* 25, pp. 29–34.

Jacquemoud, Stéphane and Verhoef, Wout and Baret, Frédéric and Bacour, Cédric and Zarco-Tejada, Pablo J and Asner, Gregory P and François, Christophe and Ustin, Susan L (2009). "PROSPECT+

SAIL models: A review of use for vegetation characterization". In: *Remote sensing of environment* 113, S56–S66.

John, Ranjeet, Jiquan Chen, Nan Lu, Ke Guo, Cunzhu Liang, Yafen Wei, Asko Noormets, Keping Ma, and Xingguo Han (2008). "Predicting plant diversity based on remote sensing products in the semi-arid region of Inner Mongolia". In: *Remote Sensing of Environment* 112.5, pp. 2018–2032.

Kingman, John Frank Charles (1992). *Poisson processes*. Vol. 3. Clarendon Press.

Laliberté, E., P. Legendre, and B. Shipley (2014). *FD: measuring functional diversity from multiple traits, and other tools for functional ecology.* R package version 1.0-12.1.

Landmann, Tobias, Hannes Feilhauer, Miaogen Shen, Jin Chen, and Suresh Raina (2019). "Hyperspectral Remote Sensing of Vegetation. Advanced Applications in Remote Sensing of Agricultural Crops and Natural Vegetation". In: ed. by Prasad Thenkabail, John Lyon, and Alfredo Huete. 2nd ed. Vol. IV. Taylor and Francis. Chap. Mapping the Distribution and Abundance of Flowering Plants Using Hyperspectral Sensing.

Lehnert, Lukas W., Hanna Meyer, Wolfgang A. Obermeier, Brenner Silva, Bianca Regeling, Boris Thies, and Jörg Bendix (2019). "Hyperspectral Data Analysis in R: The hsdar Package". In: *Journal of Statistical Software* 89.12, pp. 1–23. DOI: 10.18637/jss.v089.i12.

Lucas, Kelly L., George T. Raber, and Gregory A. Carter (2010). "Estimating vascular plant species richness on Horn Island, Mississippi using small-footprint airborne LIDAR". In: *Journal of Applied Remote Sensing* 4.1, p. 043545. DOI: 10.1117/1.3501119. URL: https://doi.org/10.1117/1.3501119.

Ludwig, Antonia D., Daniel Doktor, Reimund Goss, Severin Sasso, and Hannes Feilhauer (2022). "The leaf is always greener on the other side of the lab: Optical in-situ indicators for leaf chlorophyll content need improvement for semi-natural grassland areas". In: *Ecological Indicators* 143, p. 109424. ISSN: 1470-160X. DOI: https://doi.org/10.1016/j.ecolind.2022.109424. URL: https://www.sciencedirect.com/science/article/pii/S1470160X22008974.

Magurran, Anne E and Brian J McGill (2010). *Biological diversity: frontiers in measurement and assessment*. OUP Oxford.

Markwell, J., J. Osterman, and J. Mitchell (1995). "Calibration of the Minolta SPAD-502 leaf chlorophyll meter". In: *Photosynthesis Research* 46, pp. 467–472.

Matérn, B (1960). "Spatial variation: Meddelanden fran statens skogsforskningsinstitut". In: *Lecture Notes in Statistics* 36, p. 21.

Oldeland, Jens, Dirk Wesuls, Duccio Rocchini, Michael Schmidt, and Norbert Jürgens (2010). "Does using species abundance data improve estimates of species diversity from remotely sensed spectral heterogeneity?" In: *Ecological Indicators* 10.2, pp. 390–396.

Pacheco-Labrador, Javier et al. (2022). "Challenging the link between functional and spectral diversity with radiative transfer modeling and data". In: *Remote Sensing of Environment* 280, p. 113170.

Palmer, M.W., T. Wohlgemuth, P. Earls, J.R. Arévalo, and S.D. Thompson (2000). "Opportunities for long-term ecological research at the Tallgrass Prairie Preserve, Oklahoma". In: *Proceedings of the ILTER Regional Workshop: Cooperation in Long Term Ecological Research in Central and Eastern Europe, Budapest, Hungary*. Vol. 22.

Perez-Harguindeguy, Natalia et al. (2016). "Corrigendum to: New handbook for standardised measurement of plant functional traits worldwide". In: *Australian Journal of botany* 64.8, pp. 715–716.

Perrone, Michela et al. (2023). "The relationship between spectral and plant diversity: Disentangling the influence of metrics and habitat types at the landscape scale". In: *Remote Sensing of Environment* 293, p. 113591.

Petermann, Jana S and Oksana Y Buzhdygan (2021). "Grassland biodiversity". In: *Current Biology* 31.19, R1195–R1201.

R Core Team (2020). *R: A Language and Environment for Statistical Computing*. R Foundation for Statistical Computing. Vienna, Austria. URL: https://www.R-project.org/.

Raunkiaer, Christen et al. (1934). "The life forms of plants and statistical plant geography; being the collected papers of C. Raunkiær." In: *The life forms of plants and statistical plant geography; being the collected papers of C. Raunkiaer.*

Rocchini, D, L Dadalt, L Delucchi, M Neteler, and MW Palmer (2014). "Disentangling the role of remotely sensed spectral heterogeneity as a proxy for North American plant species richness". In: *Community Ecology* 15.1, pp. 37–43.

Rocchini, D et al. (2022). "The spectral species concept in living color". In: *Journal of geophysical research: Biogeosciences* 127.9, e2022JG007026.

Rocchini, Duccio (2007). "Effects of spatial and spectral resolution in estimating ecosystem $\alpha$-diversity by satellite imagery". In: *Remote sensing of Environment* 111.4, pp. 423–434.

Rocchini, Duccio and Chiarucci, Alessandro and Loiselle, Steven A. (2004). "Testing the spectral variation hypothesis by using satellite multispectral images". In: *Acta Oecologica* 26.2, pp. 117–120. ISSN: 1146-609X. DOI: https://doi.org/10.1016/j.actao.2004.03.008. URL: https://www.sciencedirect.com/science/article/pii/S1146609X04000311.

Rocchini, Duccio and Marcantonio, Matteo and Ricotta, Carlo (2017). "Measuring Rao's Q diversity index from remote sensing: An open source solution". In: *Ecological Indicators* 72, pp. 234–238. ISSN: 1470-160X. DOI: https://doi.org/10.1016/j.ecolind.2016.07.039. URL: https://www.sciencedirect.com/science/article/pii/S1470160X16304319.

Rossi, Christian, Mathias Kneubühler, Martin Schütz, Michael E Schaepman, Rudolf M Haller, and Anita C Risch (2021). "Remote sensing of spectral diversity: A new methodological approach to account for spatio-temporal dissimilarities between plant communities". In: *Ecological Indicators* 130, p. 108106.

— (2022). "Spatial resolution, spectral metrics and biomass are key aspects in estimating plant species richness from spectral diversity in species-rich grasslands". In: *Remote Sensing in Ecology and Conservation* 8.3, pp. 297–314. DOI: https://doi.org/10.1002/rse2.244. eprint: https://

zslpublications.onlinelibrary.wiley.com/doi/pdf/10.1002/rse2.244. URL: https://zslpublications.onlinelibrary.wiley.com/doi/abs/10.1002/rse2.244.

Schiefer, Felix, Sebastian Schmidtlein, and Teja Kattenborn (2021). "The retrieval of plant functional traits from canopy spectra through RTM-inversions and statistical models are both critically affected by plant phenology". In: *Ecological Indicators* 121. ISSN: 1470-160X. DOI: doi.org/10.1016/j.ecolind.2020.107062. URL: https://www.sciencedirect.com/science/article/pii/S1470160X20310013.

Schmidtlein, Sebastian and Fabian Ewald Fassnacht (2017). "The spectral variability hypothesis does not hold across landscapes". In: *Remote sensing of environment* 192, pp. 114–125.

Schneider, Fabian D, Felix Morsdorf, Bernhard Schmid, Owen L Petchey, Andreas Hueni, David S Schimel, and Michael E Schaepman (2017). "Mapping functional diversity from remotely sensed morphological and physiological forest traits". In: *Nature communications* 8.1, p. 1441.

Schweiger, Anna K, Jeannine Cavender-Bares, Philip A Townsend, Sarah E Hobbie, Michael D Madritch, Ran Wang, David Tilman, and John A Gamon (2018). "Plant spectral diversity integrates functional and phylogenetic components of biodiversity and predicts ecosystem function". In: *Nature Ecology & Evolution* 2.6, pp. 976–982.

Shen, Miaogen, Jin Chen, Xiaolin Zhu, and Yanhong Tang (2009). "Yellow flowers can decrease NDVI and EVI values: Evidence from a field experiment in an alpine meadow". In: *Canadian journal of remote sensing* 35.2, pp. 99–106.

Siefert, Andrew et al. (2015). "A global meta-analysis of the relative extent of intraspecific trait variation in plant communities". In: *Ecology Letters* 18.12, pp. 1406–1419. DOI: 10.1111/ele.12508. eprint: https://onlinelibrary.wiley.com/doi/pdf/10.1111/ele.12508. URL: https://onlinelibrary.wiley.com/doi/abs/10.1111/ele.12508.

Simpson, Edward H (1949). "Measurement of diversity". In: *nature* 163.4148, pp. 688–688.

Thornley, Rachael, France Gerard, Kevin White, and Anne Verhoef (2023). "Prediction of Grassland Biodiversity Using Measures of Spectral Variance: A Meta-Analytical Review". In: *Remote Sensing* 15.3. ISSN: 2072-4292. DOI: 10.3390/rs15030668. URL: https://www.mdpi.com/2072-4292/15/3/668.

Thornley, Rachael, France F Gerard, Kevin White, and Anne Verhoef (2022). "Intra-annual taxonomic and phenological drivers of spectral variance in grasslands". In: *Remote Sensing of Environment* 271, p. 112908.

Torresani, Michele, Hannes Feilhauer, Duccio Rocchini, Jean-Baptiste Féret, Marc Zebisch, and Giustino Tonon (2021). "Which optical traits enable an estimation of tree species diversity based on the Spectral Variation Hypothesis?" In: *Applied Vegetation Science* 24.2, e12586. DOI: 10.1111/avsc.12586. eprint: https://onlinelibrary.wiley.com/doi/pdf/10.1111/avsc.12586. URL: https://onlinelibrary.wiley.com/doi/abs/10.1111/avsc.12586.

Verhoef, W (1985). "Earth observation modeling based on layer scattering matrices". In: *Remote sensing of environment* 17.2, pp. 165–178.

Verhoef, W, L Jia, Q Xiao, and Z Su (2007). "Unified Optical-Thermal Four-Stream Radiative Transfer Theory for Homogeneous Vegetation Canopies". In: *IEEE Transactions on Geoscience and Remote Sensing* 45.6, pp. 1808–1822. DOI: 10.1109/TGRS.2007.895844.

Verhoef, W (1984). "Light scattering by leaf layers with application to canopy reflectance modeling: The SAIL model". In: *Remote sensing of environment* 16.2, pp. 125–141.

Wang, Ran and John Gamon (2019). "Remote sensing of terrestrial plant biodiversity". In: *Remote Sensing of Environment* 231, p. 111218. ISSN: 0034-4257. DOI: 10.1016/j.rse.2019.111218.

Wang, Ran, John A. Gamon, Rebecca A. Montgomery, Philip A. Townsend, Arthur I. Zygielbaum, Keren Bitan, David Tilman, and Jeannine Cavender-Bares (2016). "Seasonal variation in the NDVI–species richness relationship in a prairie grassland experiment (Cedar Creek)". In: *Remote Sensing* 8.2, p. 128.

Wang, Ran, John A. Gamon, Anna K. Schweiger, Jeannine Cavender-Bares, Philip A. Townsend, Arthur I. Zygielbaum, and Shan Kothari (2018a). "Influence of species richness, evenness, and composition on optical diversity: A simulation study". In: *Remote Sensing of Environment* 211, pp. 218–228. ISSN: 0034-4257. DOI: 10.1016/j.rse.2018.04.010. URL: https://www.sciencedirect.com/science/article/pii/S003442571830155X.

Wang, Ran, A John, J Cavender-Bares, PA Townsend, and AI Zygielbaum (2018b). "The spatial sensitivity of the spectral diversity–biodiversity relationship: an experimental test in a prairie grassland". In: *Ecological Applications* 28.2, pp. 541–556.

Weiner, Jacob, Peter Stoll, H Muller-Landau, and A Jasentuliyana (2001). "The effects of density, spatial pattern, and competitive symmetry on size variation in simulated plant populations". In: *The American Naturalist* 158.4, pp. 438–450.

Zhao, Yujin, Yihan Sun, Wenhe Chen, Yanping Zhao, Xiaoliang Liu, and Yongfei Bai (2021). "The potential of mapping grassland plant diversity with the links among spectral diversity, functional trait diversity, and species diversity". In: *Remote Sensing* 13.15, p. 3034.

# List of Figures

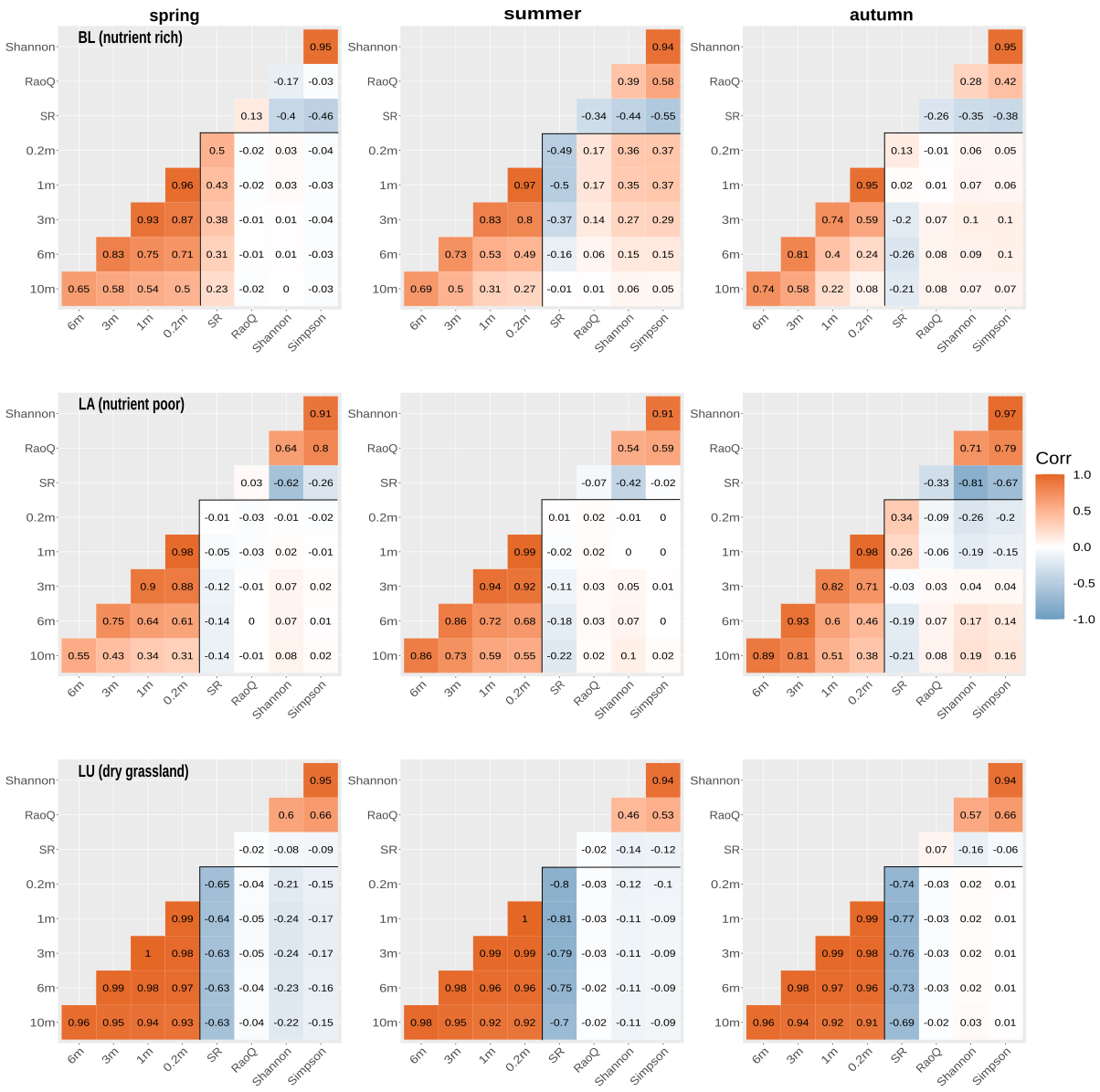


Figure 4: Correlograms representing the bivariate relationships (R-values) between spectral diversity (mED) and different taxonomic diversity indices calculated for each of the grassland simulations based on in-situ species and trait data. Black numbers show Pearson's correlation coefficient. The lower triangle shows the correlations between the mED of the different spatial resolutions, the upper triangle shows the correlations between the different diversity indices (taxonomic and functional). R-values within the grey box show the correlations between different taxonomic and functional indices and spectral diversity for different spatial resolutions. Labels: 'Simpson' - Simpson-Index, 'Shannon' - Shannon Index, 'RaoQ' - Rao's quadratic entropy, 'SR' - Species Richness. Sites: BL - Bad Lauchstädt, LA - Luppeaue, LU - Lunzberge. See Figure 18 for spectral Rao's Q.

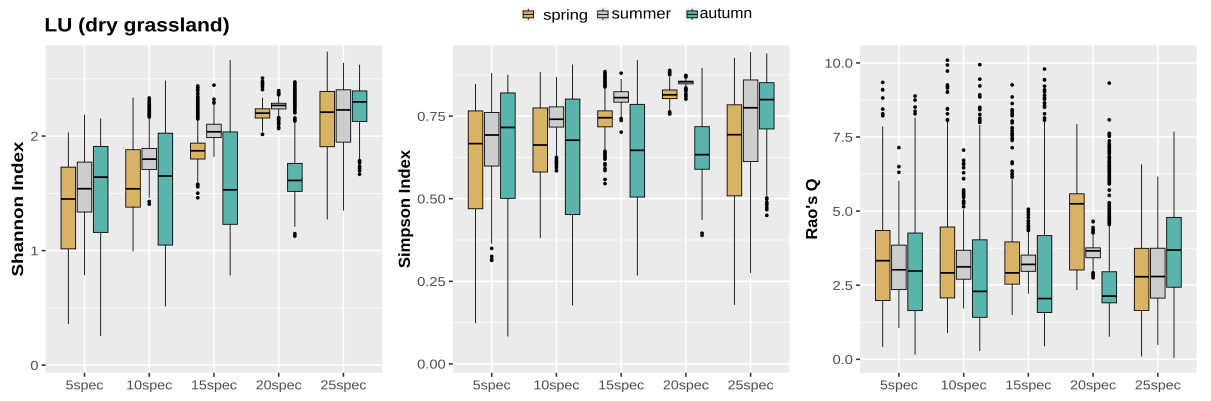


Figure 5: Taxonomic and functional diversity indices per diversity level for the LU site as an example. Indices were calculated for each of the 1000 grassland simulations per diversity level and for each season (in different colours). The species and trait data is based on in-situ measurements from the study sites. Season-specific results from the linear regression model between the respective index and species numbers are written in each panel. LU - Lunzberge.

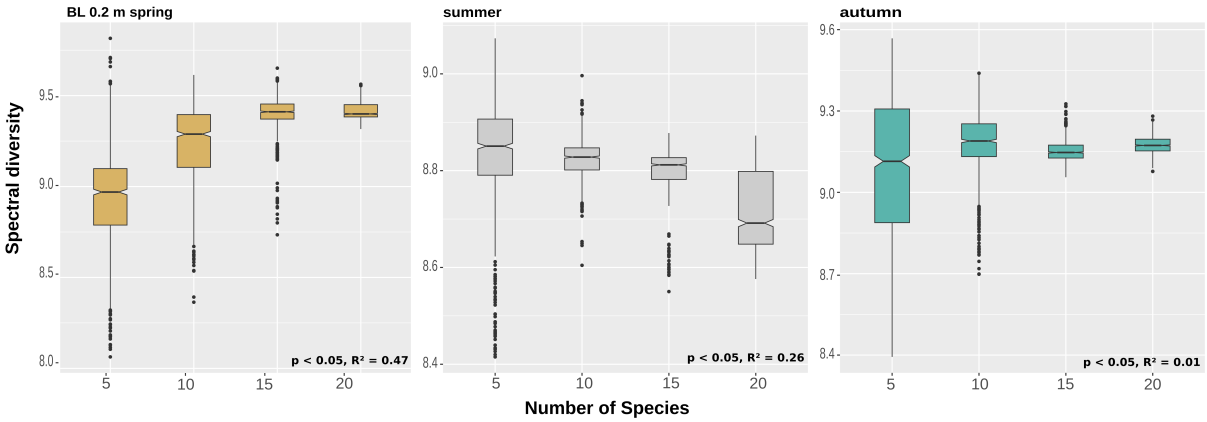


Figure 6: Spectral diversity (mED in log+1) per diversity level. Depicted is the Bad Lauchstädt (BL site) site in spring, summer and autumn as an example. Each box contains the mED for all 1000 grassland simulations per diversity level (5 species to 20 species) in the finest resolution (0.2 m pixel size). Results from the linear regression model between mED and species numbers are written in each panel. The reader is referred to the remaining plots of the other study sites in the supplement (Fig. A.16).

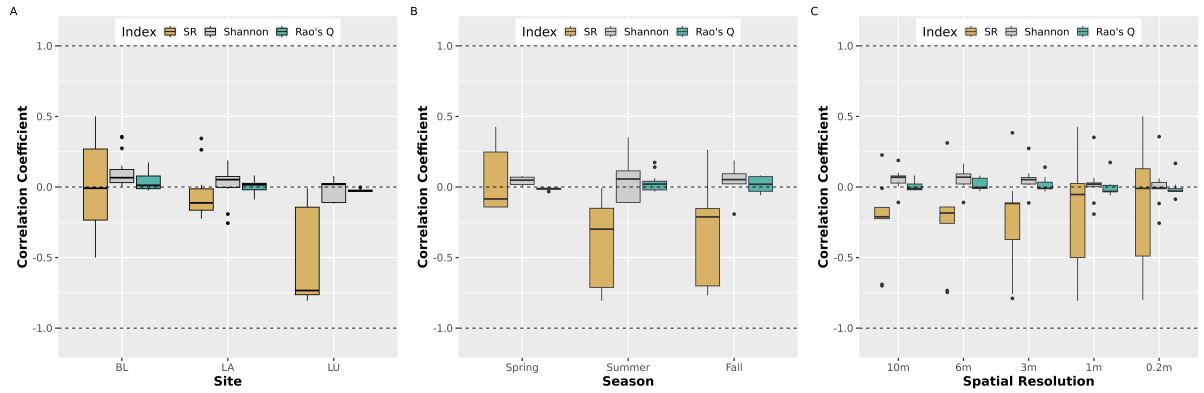


Figure 7: Correlation coefficients for taxonomic (Number of Species, Shannon-Index) and functional diversity (Rao's Q) indices with spectral diversity (mED) from different perspectives. Boxes show the R-values for the respective index and spectral diversity for (A) the single sites, including all seasons and spatial resolutions, (B) single seasons, including all sites and spatial resolutions, and (C) single spatial resolutions, including all sites and seasons. BL - Bad Lauchstädt (nutrient-rich), LA - Luppeaue (nutrient-poor), LU - Lunzberge (dry grassland).

.

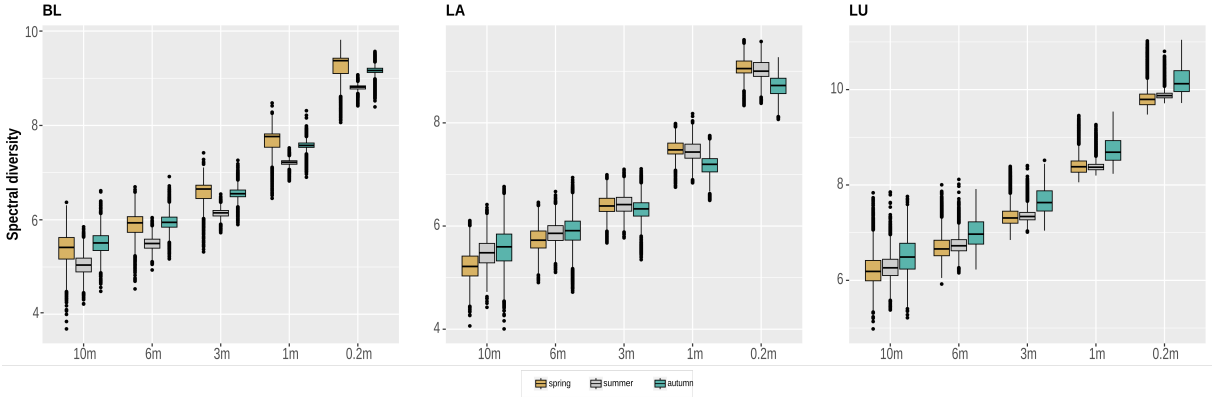


Figure 8: Spectral diversity per spatial resolution for each site and season. Each box contains the spectral diversity of all grassland simulations in the respective spatial resolution (i.e. all diversity levels combined per spatial resolution). The spectral resolution remained unchanged across the different spatial resolutions (hyperspectral, 188 bands). BL - Bad Lauchstädt (nutrient-rich), LA - Luppeaue (nutrient-poor), LU - Lunzberge (dry grassland).

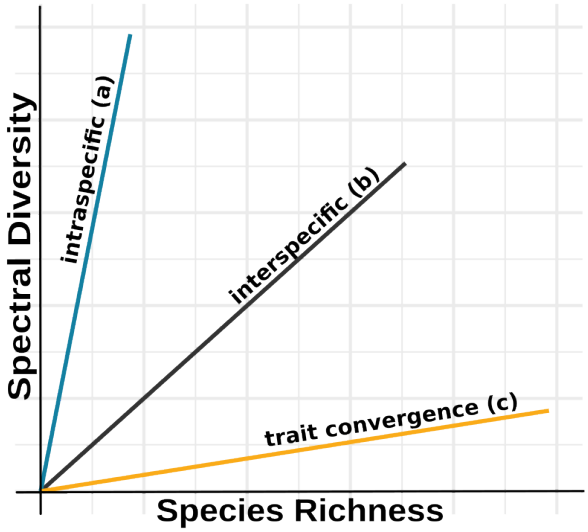


Figure 9: Schematic overview on the influence of different scenarios of trait expressions on the relationship between spectral diversity and SR. The figure was inspired by results from Díaz, Sandra and Cabido, Marcelo (2001) that presented a detailed analysis on the mismatch between SD and FD considering different settings. We expanded their concept to the spectral domain. Case (a) represents high intraspecific trait variability at low levels of SR, e.g. caused by strong environmental heterogeneity in an area. High spectral diversity leads to an overestimation of SR in this case. Case (b) shows high interspecific trait variability, increasing with increasing SR. In this case, the link between spectral diversity and SR is given. Case (c) represents high trait convergence, i.e. different species develop similar sets of traits in the same area. FD is low and leads to low spectral diversity that does not represent high SR. Note that environmental heterogeneity or other factors driving spectral diversity are not included in this graph. These can further lead to an overestimation of spectral diversity and bias the spectral-to-species diversity relationship.

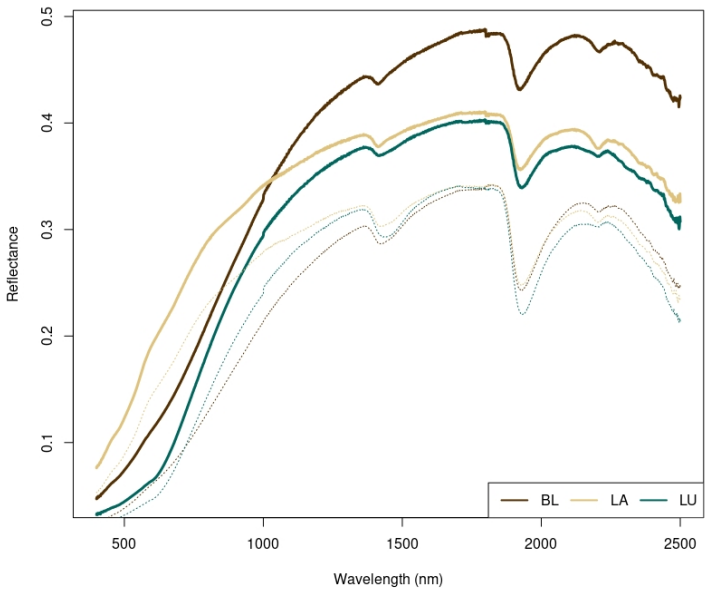


Figure 10: Soil reflectance spectra from all field sites. Samples were collected from the uppermost layer and dried at 40 °C for at least 48 h. Afterwards, the samples were sieved to a grain size of 1 mm. Soil reflectance was measured using the contact probe of a field spectrometer (ASD FieldSpec 4®, Malvern Panalytical, UK) fixed to a stand. Measuring height was adjusted to the diameter of the measured area (diameter = 5 cm, height = 10 cm) as well as the incidence angle of the halogen lamp (< = 30°). A correction curve was recorded using a white reference panel with 95% reflectance prior to the soil reflectance measurements. The single samples were measured three times and turned approx 120° after each measurement. Each run consists of three full spectral records (from 350 - 2500 nm wavelength), while the outcome of reflectance values at individual wavelengths is calculated as the mean of 25 measurements at the exact same position of the spectrum. Samples were first measured dry (dotted line) and then re-wetted (solid line) to 10% mass content $H_2O$. Site codes: BL - Bad Lauchstädt (nutrient-rich), LA - Luppeaue (nutrient-poor) , LU - Lunzberge (dry grassland).

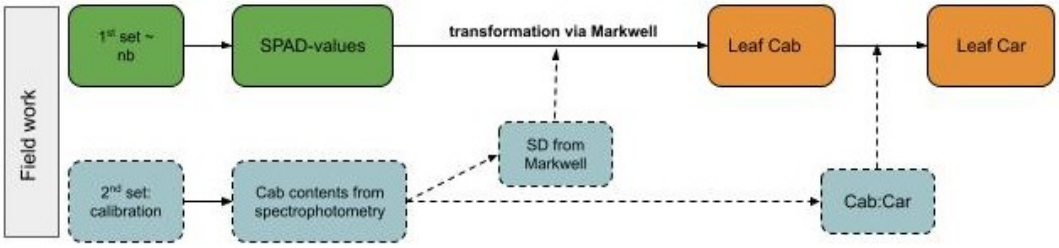


Figure 11: From SPAD-values in the field to total leaf chlorophyll (Cab) and carotenoid (Car) contents using two sets of samples: A larger set of samples (n= ) that were measured with the SPAD-chlorophyllmeter and a second set (n = 160) for calibration. Total leaf Cab was calculated from SPAD-values under consideration of (1) the deviations between measured Cab based on spectrophotometry and transformed SPAD-values based on Markwell et al. (1995) ('SD from Markwell'). Further, taking into account (2) the ratio between Cab and Car ('Cab:Car') from the calibration set to derive final car for the first sample set.

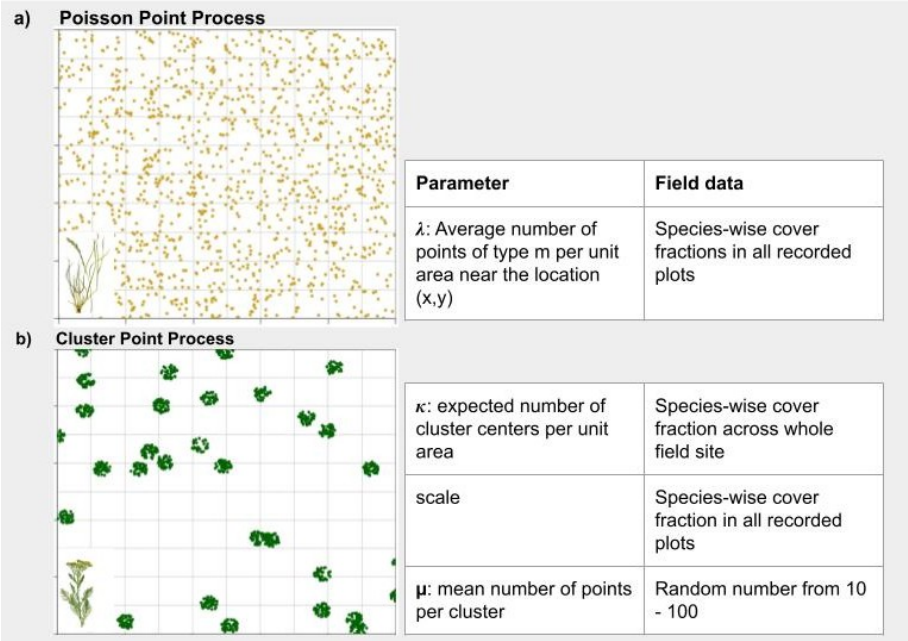


| Parameter | Field data |
|---|---|
| $\lambda$: Average number of points of type m per unit area near the location (x,y) | Species-wise cover fractions in all recorded plots |

| | |
|---|---|
| $\kappa$: expected number of cluster centers per unit area | Species-wise cover fraction across whole field site |
| scale | Species-wise cover fraction in all recorded plots |
| $\mu$: mean number of points per cluster | Random number from 10 - 100 |

Figure 12: Realisation of two types of point pattern distributions for approximately 1200 points in both cases (for better illustration). a) Poisson point pattern process for homogeneously distributed species (e.g. *Lolium perenne*). The intensity function was parameterised with the cover fractions of the individual species that were estimated during field work. b) A Matern cluster process for species that grow clustered (e.g. *T. vulgare*). The table shows the field data that have been used to parameterise the respective density functions.

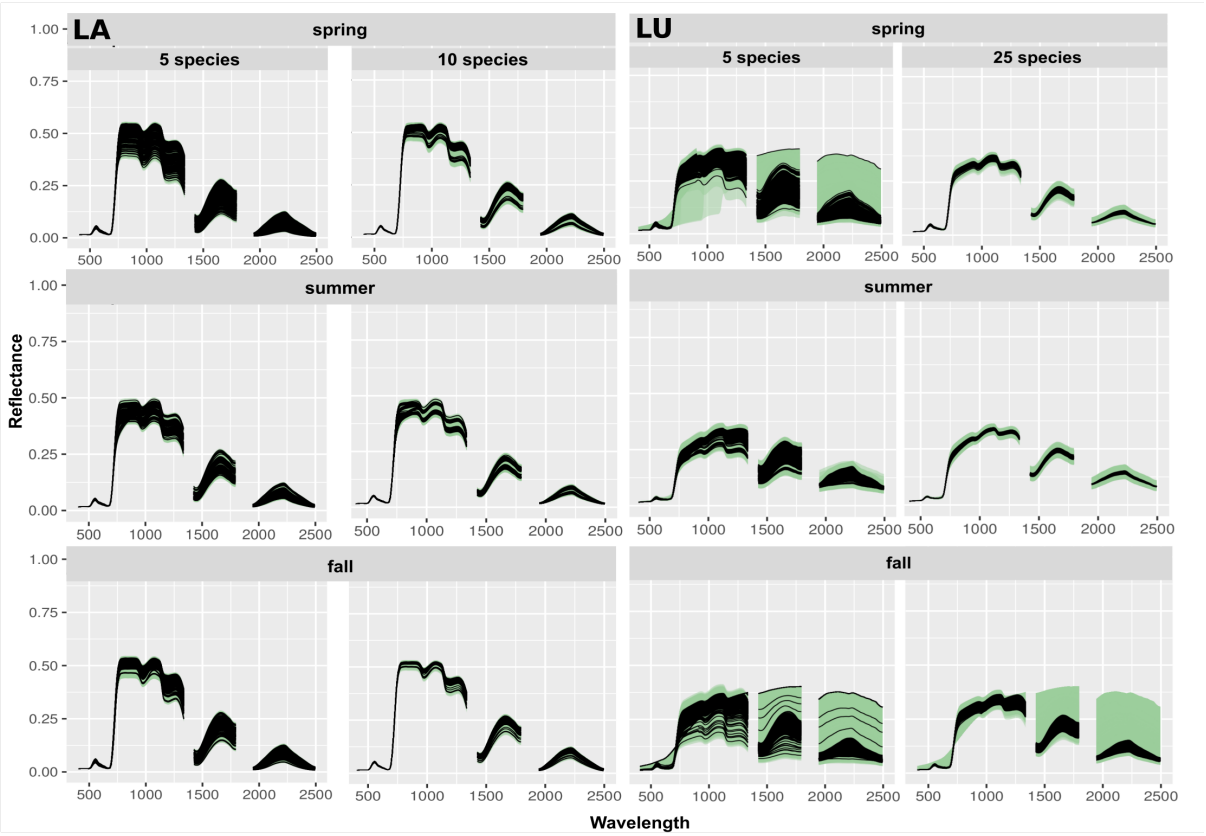


Figure 13: Median reflectance spectra of the 1000 simulated grassland communities for the lowest and highest species numbers in each season. Black lines depict the median spectrum of a single grassland simulation in the finest spatial resolution, i.e. the median spectrum of 22500 pixels. Green areas show the upper and lower quartiles (75 % and 25 %) of the pixel-wise spectra from the single simulations. Panels in the two columns on the left side show the spectra of LA, the two columns on the right side show the spectra of LU. LA - Luppeaue (nutrient-poor), LU - Lunzberge (dry-grassland).

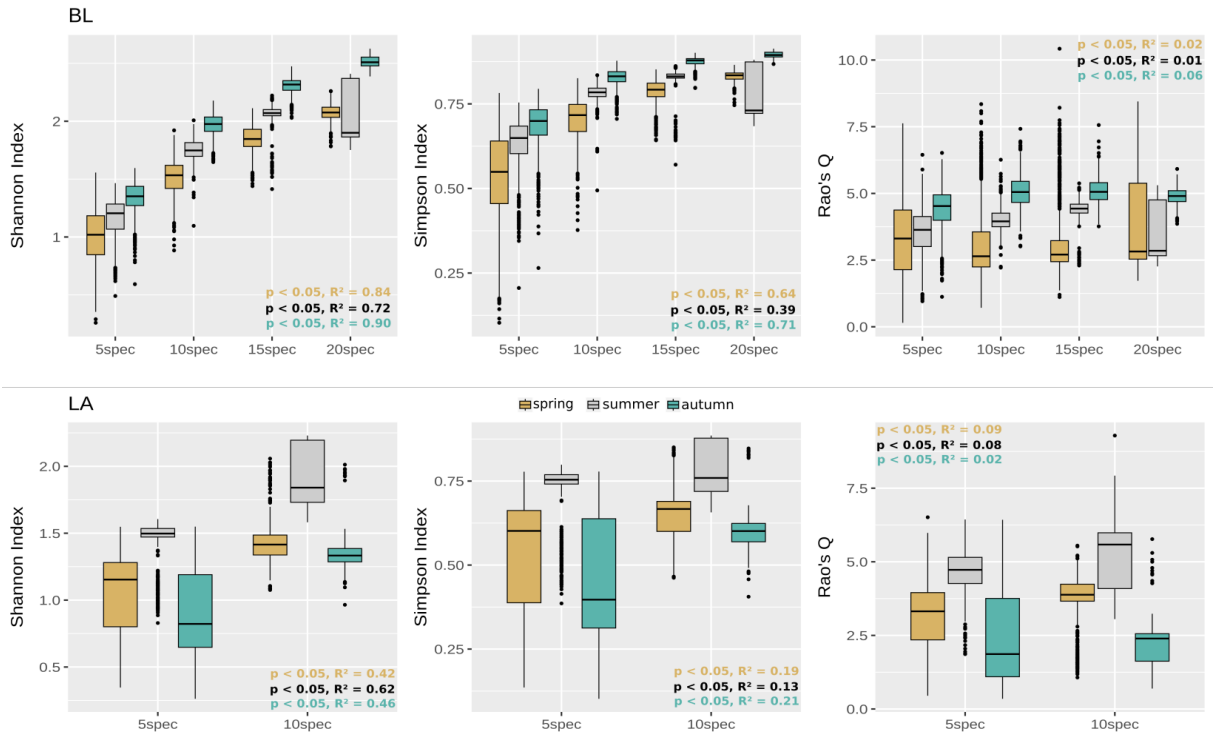


Figure 14: Taxonomic and functional diversity indices per site and season. Indices were calculated for each of the 1000 grassland simulations per diversity level. In order to calculate them for every single grassland simulation, we attached species-specific trait data to the individual points in the two dimensional grassland communities. The species and trait data is based on in-situ measurements from the study sites. Site codes: BL - Bad Lauchstädt (nutrient-rich), LA - Luppeaue (nutrient-poor).

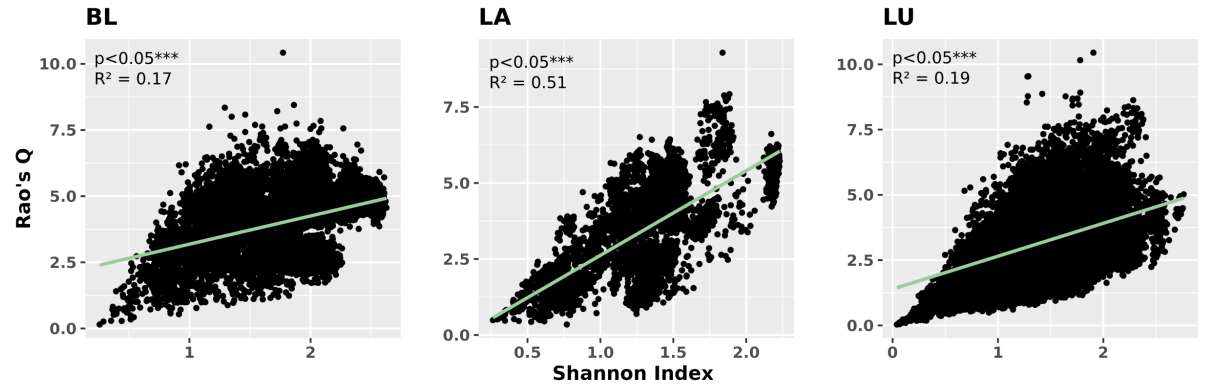


Figure 15: The relationship between Rao's Q (Functional diversity) and Shannon index (Species diversity) per site. Data was summarised for all seasons in one plot. Overall, the linear regression model suggests that there is a significant relationship between Rao's Q and Shannon index, although in BL and LA the model explains only a small proportion of the variance in Rao's Q. Site codes: BL - Bad Lauchstädt (nutrient-rich), LA - Luppeaue (nutrient-poor), LU - Lunzberge (dry grassland).

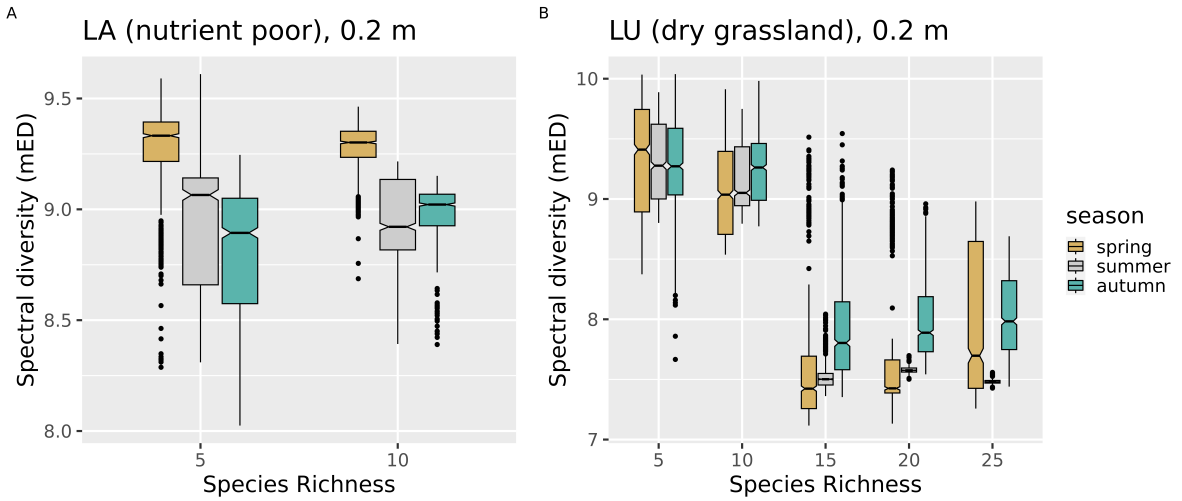


Figure 16: Spectral diversity (mED in log+1) per diversity level for the sites LA and LU across all seasons. Each box contains the mED for all 1000 grassland simulations per diversity level (5 species to 25 species) in the finest resolution (0.2 m pixel size). The relationship between mED and diversity level is not stable across the sites and seasons.

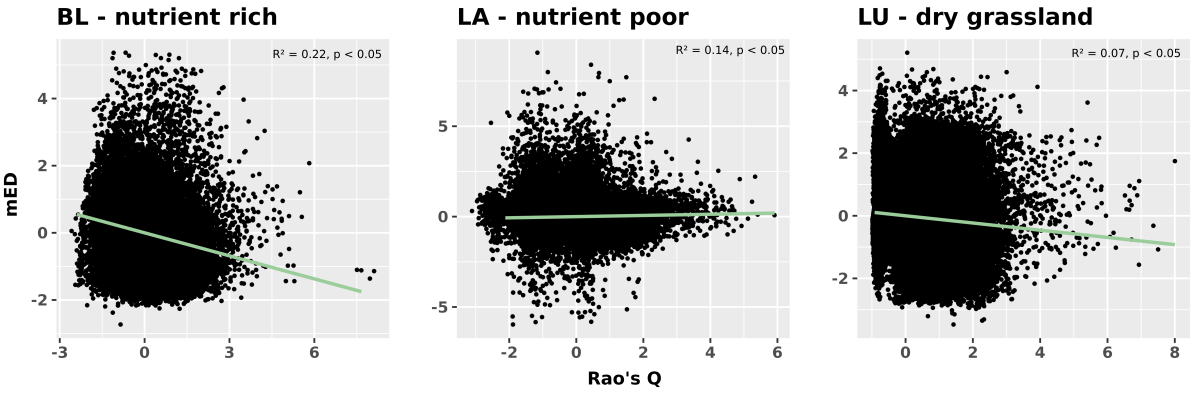


Figure 17: Correlation between the two metrics for spectral diversity. Spectral Rao's Q and mED have been scaled before the linear regression model was applied. Correlations were all non significant and $R^2$-values were low (p ¡ 0.05 in all cases, see plot panels for site-specific $R^2$-values.)

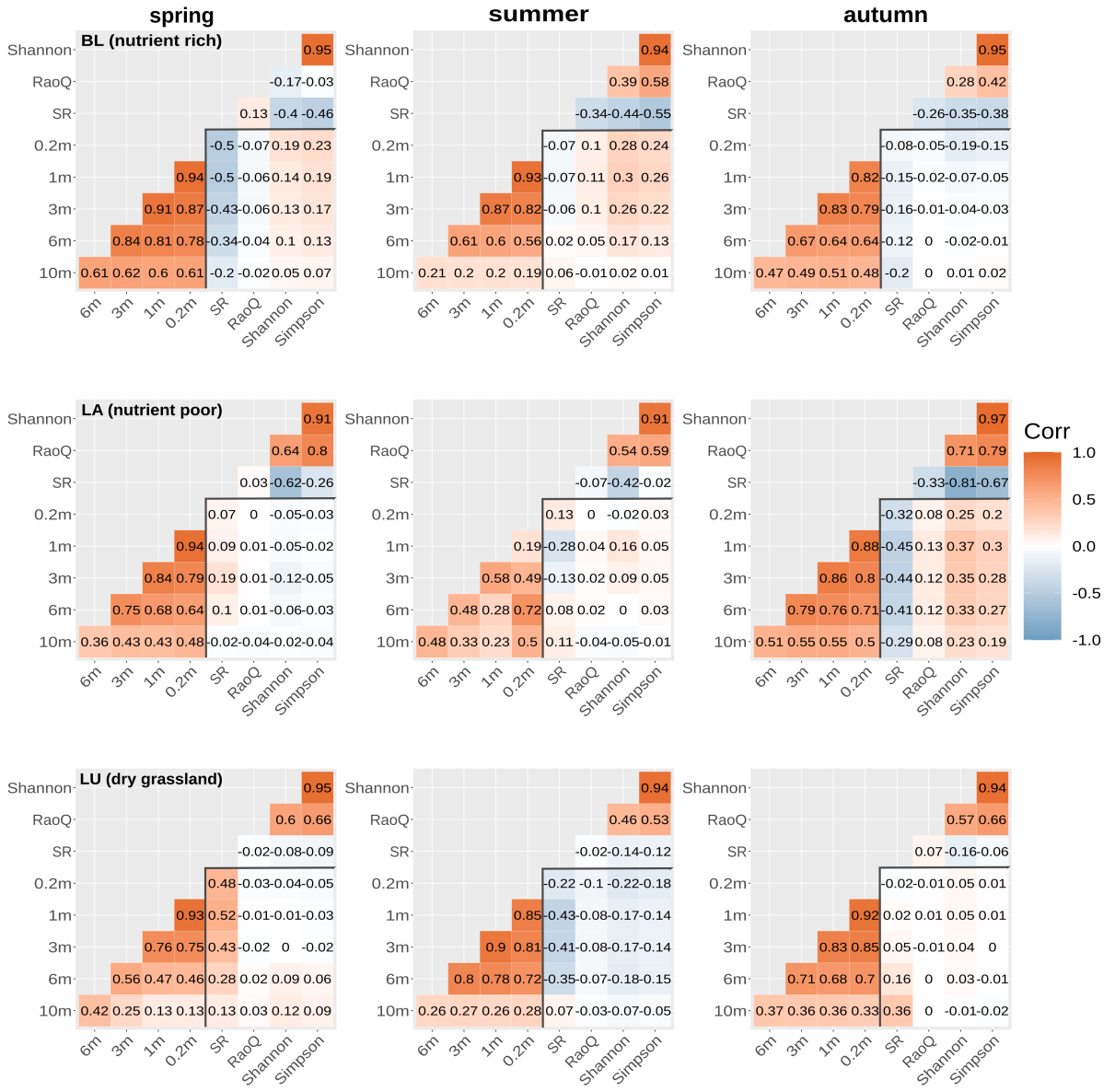


Figure 18: Correlograms representing the bivariate relationships (R-values) between spectral diversity (Rao's Q) and different taxonomic diversity indices calculated for each of the grassland simulations based on in-situ species and trait data. Black numbers show Pearson's correlation coefficient. The lower triangle shows the correlations between spectral Rao's Q of the different spatial resolutions, the upper triangle shows the correlations between the different diversity indices (taxonomic and functional). R-values within the grey box show the correlations between different taxonomic and functional indices and spectral diversity for different spatial resolutions. Labels: 'Simpson' - Simpson-Index, 'Shannon' - Shannon Index, 'RaoQ' - Rao's quadratic entropy, 'SR' - Species Richness. Sites: BL - Bad Lauchstädt, LA - Luppeaue, LU - Lunzberge.